Oxidized polystyrene surfaces produced by plasma and neutral beam methods : an x-ray photoelectron and surface derivatization study
by Terry Lee Thompson

A thesis submitted in partial fulfillment of the requirements for the degree i of Master of Science in Chemistry
Montana State University

Abstract:
Plasma treatments of polymers are commonly used to alter surface chemical properties, such as surface free energy, reactivity, adhesiveness, and biocomp atability. This study was conducted to investigate the use of neutral molecular beams for controlled surface modification. Detailed investigations of the chemistry of polymer surfaces that have been oxidized by neutral molecular beams have not previously been investigated in depth. Oxygen plasma modifications of polystyrene surfaces have been extensively investigated. Polystyrene was used as a model surface to compare the effects of neutral oxygen beams and oxygen plasmas on polymer surfaces. In an oxygen plasma environment, the surface is exposed to ions, ozone, atoms, electrons, excited states of molecular and atomic oxygen, and to a broad electromagnetic spectrum. The resultant chemistry can be difficult to control. Beams composed primarily of energetic oxygen atoms and molecules may offer the possibility to achieve more controlled surface chemistries.

Polystyrene samples were exposed to hyperthermal neutral oxygen beams composed of an approximately 60/40 mix of oxygen atoms to oxygen molecules traveling at an average velocity of 8 km/sec. Samples were also exposed to radio-frequency oxygen plasmas under commonly used operating parameters. X-ray photoelectron spectroscopy (XPS), surface chemical derivatization, and scanning electron microscopy (SEM) were used to characterize the surfaces.

Both modification methods resulted in similar amounts of surface oxidation that increased with progressively greater intensity or duration of exposure, with different distributions of carbon-oxygen bonding environments. The molecular beam produced unique metastable species that lasted up to two weeks. Once the surfaces had aged, the different beam exposure durations had nearly identical chemistry. The beam exposure resulted in the formation of sub-micron surface features that increased in number with increased exposure duration, while the plasma exposure did not affect surface roughness. The surface roughness could be varied independently of surface chemistry with the molecular beam. Plasma exposure resulted in the destruction of the aromatic structure of the polystyrene, while the beam exposure left the aromatic character intact. Surface derivatization was not effective in obtaining accurate quantitative results in systems with a variety of functionalities in low concentrations because of cross-reaction and yield problems.

OXIDIZED POLYSTYRENE SURFACES PRODUCED BY PLASMA AND NEUTRAL BEAM METHODS: AN X-RAY PHOTOELECTRON AND SURFACE DERIVATIZATION STUDY

by

Terry Lee Thompson

A thesis submitted in partial fulfillment
of the requirements for the degree

of

Master of Science

in

Chemistry

MONTANA STATE UNIVERSITY-BOZEMAN
Bozeman, Montana

December 1997

APPROVAL

of a thesis submitted by

Terry Lee Thompson

This thesis has been read by each member of the thesis committee and has been found to be satisfactory regarding content, English usage, format, citations, bibliographic style, and consistency, and is ready for submission to the College of Graduate Studies.

12/3/97
Date

Timothy K. Minton
Chairperson, Graduate Committee

Approved for the Major Department

Dec. 4, 1997
Date

David W. Dooley
Head, Major Department

Approved for the College of Graduate Studies

12/11/97
Date

Joseph J. Fedock
Graduate Dean

STATEMENT OF PERMISSION TO USE

In presenting this thesis as partial fulfillment of the requirements for a master's degree at Montana State University-Bozeman, I agree that the library shall make it available to borrowers under the rules of the library.

If I have indicated my intention to copyright this thesis by including a copyright notice page, copying is allowable only for scholarly purposes, consistent with "fair use" as prescribed in the U.S. Copyright Law. Requests for permission for extended quotation from or reproduction of this thesis in whole or in parts may be granted only by the copyright holder.

Terry L Thompson
Signature

12/3/97
Date

ACKNOWLEDGEMENTS

I would like to extend my gratitude to my advisor Dr. Tim Minton and to Dr. Bonnie Tyler for their supervision, support, and advice on this project.

I would also like to thank the following individuals for their contributions: Lorna Mitson for preparation and analysis of plasma-exposed samples, Dr. Patrick Shamberger for preparation of plasma-exposed samples and XPS analysis of plasma- and beam-exposed samples, Alex Ide for preparation of beam-exposed samples, and Kristina Bjorklund for development of derivatization methods.

I would like to thank the organizations involved in supporting this project: the National Science Foundation through a cooperative agreement with the Center for Biofilm Engineering and Montana State University, and a grant from the Department of Defense Experimental Program for the Stimulation of Competitive Research (DEPSCoR) administered by the Air Force Office of Scientific Research, the Image and Chemical Analysis Laboratory at Montana State University, where the XPS and SEM data were collected.

TABLE OF CONTENTS

TABLE OF CONTENTS – Cont.

LIST OF TABLES

LIST OF FIGURES

LIST OF FIGURES - Cont.

LIST OF FIGURES – Cont.

ABSTRACT

Plasma treatments of polymers are commonly used to alter surface chemical properties, such as surface free energy, reactivity, adhesiveness, and biocompatability. This study was conducted to investigate the use of neutral molecular beams for controlled surface modification. Detailed investigations of the chemistry of polymer surfaces that have been oxidized by neutral molecular beams have not previously been investigated in depth. Oxygen plasma modifications of polystyrene surfaces have been extensively investigated. Polystyrene was used as a model surface to compare the effects of neutral oxygen beams and oxygen plasmas on polymer surfaces. In an oxygen plasma environment, the surface is exposed to ions, ozone, atoms, electrons, excited states of molecular and atomic oxygen, and to a broad electromagnetic spectrum. The resultant chemistry can be difficult to control. Beams composed primarily of energetic oxygen atoms and molecules may offer the possibility to achieve more controlled surface chemistries.

Polystyrene samples were exposed to hyperthermal neutral oxygen beams composed of an approximately 60/40 mix of oxygen atoms to oxygen molecules traveling at an average velocity of 8 km/sec. Samples were also exposed to radio-frequency oxygen plasmas under commonly used operating parameters. X-ray photoelectron spectroscopy (XPS), surface chemical derivatization, and scanning electron microscopy (SEM) were used to characterize the surfaces.

Both modification methods resulted in similar amounts of surface oxidation that increased with progressively greater intensity or duration of exposure, with different distributions of carbon-oxygen bonding environments. The molecular beam produced unique metastable species that lasted up to two weeks. Once the surfaces had aged, the different beam exposure durations had nearly identical chemistry. The beam exposure resulted in the formation of sub-micron surface features that increased in number with increased exposure duration, while the plasma exposure did not affect surface roughness. The surface roughness could be varied independently of surface chemistry with the molecular beam. Plasma exposure resulted in the destruction of the aromatic structure of the polystyrene, while the beam exposure left the aromatic character intact. Surface derivatization was not effective in obtaining accurate quantitative results in systems with a variety of functionalities in low concentrations because of cross-reaction and yield problems.

CHAPTER 1

INTRODUCTION

Surface modification and surface engineering are very important for many scientific research areas. Modification of a surface may be advantageous when a bulk material that has some desirable property such as high strength, low cost, or durability is lacking in a surface property that is desired, like adhesion, biocompatability, or wear resistance. The surface can be treated to obtain the desired surface property while maintaining the desirable properties of the bulk material. Surface modification plays an important role in the search for biologically inert or compatible polymer based materials that are placed in biological environments both long term and permanently [1,2]. For example, the introduction of hydrophilic groups onto the surface of a synthetic implant device reduces the surface induced aggregation of blood platelets on the surface which is believed to initiate events that lead to a negative physiological response [26]. Surface modification also plays a major role in the composite materials field. For example, fibers are treated both to effect processability and their adhesion to

the matrix material, which alters end product properties [3,4]. The largest single use of plastics is for packaging, which often require treatment to achieve satisfactory adhesion of printing and coatings [5].

There are many ways a surface can be modified. Polymer surfaces can be oxidized by exposure to wet chemical oxidizing agents such as chromic acid [27]. They also can be oxidized by environmental exposure to light [8,9]. Exposure to corona discharges is widely used to enhance the adhesion of inks to polyethylene in many commercial applications [28]. Plasma techniques are widely used in many industries. Plasma etching, plasma deposition and polymerization are widely used in the manufacture of integrated circuits [29]. Radio frequency glow discharge oxygen plasmas are a common method used to modify polymer surfaces. In an oxygen plasma environment, the surface is exposed to ions, ozone, atoms, electrons, metastable excited states of molecular and atomic oxygen, and to a broad electromagnetic spectrum [6]. This can make control of the resultant chemistry difficult.

In this study, beams of energetic oxygen atoms and molecules are being investigated as an alternative method to alter surface chemical properties. Polystyrene was used as a model surface to compare the neutral beam technique with plasma oxidation because the plasma oxidation of polystyrene surfaces has been extensively studied [6,7,8,9,10,11]. The interest in the interaction of energetic oxygen atoms with surfaces has mainly been driven by the space effects community. Oxygen atoms present in

low earth orbit (LEO) undergo impact with spacecraft that are moving at orbital velocities of approximately 8 km/sec. These interactions result in significant erosion and oxidation of the materials of the spacecraft [30]. Investigations of the chemistry involved in the oxidation of Kapton and several fluorocarbon polymers have been performed by exposure to atomic oxygen in low Earth orbit on the space shuttle [31]. Beams of atomic oxygen are often used for laboratory studies of space environmental effects [32].

Plasma and hyperthermal neutral molecular beams present two very different exposure environments. Unlike plasmas, where the species present and their kinetic energies are difficult to measure and are not commonly measured during sample exposure. The neutral beams provide the opportunity for easy measurement of the species present and their energies. The oxygen molecular beam used in this study has two main components: hyperthermal neutral oxygen atoms and molecules that have variable velocities in the range of 3-9 km/sec, corresponding to O-atom kinetic energies of approximately 0.7 to 9 eV. The oxygen plasma environment presents many neutral and ionic species with a myriad of excited states and near thermal energies of approximately 0.05 eV for neutrals and energies up to 10^3 eV for ions. Unlike plasmas, beam exposure presents little opportunity for charging effects and bombardment damage with more control over surface temperature. The neutral molecular beam also has good directional control.

In a plasma environment, directional control is potentially good for ionic species.

The polystyrene monomer unit consists of a two carbon backbone with a benzyl ring attached. Exposure of polystyrene surfaces to beams of energetic oxygen atoms and to oxygen plasmas results in the incorporation of oxygen into the polymer surface. The surfaces have been characterized by X-ray photoelectron spectroscopy (XPS) and derivatization techniques that represent the bulk of the work on this thesis. Scanning electron microscopy (SEM) was used to examine surface topography.

CHAPTER 2

EXPERIMENTAL METHODS

Sample Preparation

Polystyrene

Polystyrene (PS) samples used for surface modification were from commercially available 8.5x11 inch sheets provided by Plaskolyte (Columbus, OH). The sheets had a thickness of 0.93 mm with an average molecular weight of approximately 100,000. The polystyrene sheet was cut into 0.5 inch disks. The disks were rinsed with hexane for approximately 20-30 seconds and sonicated in methanol for 5 minutes and finally patted dry. Initial beam samples were soaked in methanol for 15 minutes instead of being sonicated. Both solvents used were HPLC grade, Fisher Scientific, Fail Lawn, NJ. The samples were immediately placed in the plasma or beam apparatus for surface modification. Control samples were analyzed immediately after cleaning.

Reference Polymers

Reference polymer films were prepared to investigate the surface derivatization reactions. Polymers were purchased from either Aldrich Chemical Co. (Milwaukee, WI) or Polysciences Inc. (Warrington, PA).

Poly(vinyl methyl ketone) (PVMK) had a MW of 500,000, Poly(acrylic acid) (PAA) had a MW of 250,000, and Poly(vinyl alcohol) (PVA) had a MW of 50,000-85,000. Poly(epoxy propyl methacrylate) was received as a 10% by weight solution in methyl ethyl ketone.

Solutions of the dry polymers were prepared as follows. Polymer was weighed in a capped glass vial and solvent was added to make a desired weight percentage solution. Guidelines for solvents and weight percentages were taken from reference 21. The vials used were 20-ml scintillation vials: borosilicate glass with polypropylene lined caps (Fisher Scientific, Pittsburg, PA). The analytical scale used was a Mettler AE 200. Polymer solutions were filtered with Millex LCR 0.5 micrometer filters for organic and aqueous solvents. PVMK was dissolved in a 50/50 volume mixture of tetrahydrofuran (99.9+%, Sigma-Aldrich) and chloroform (HPLC grade, Fisher Scientific). The final solution had a 2% weight composition of polymer to solution. PAA was dissolved in methanol to make a 1.6% by weight solution. PVA was dissolved in nano-pure water to make a 1.2% by weight solution.

The polymer solutions were spin-cast onto clean 12 mm glass cover slips/disks. The glass substrates had been previously cleaned by sonication

in acetone in a Branson 2210 Ultrasonic Cleaner. The solutions were spin-cast using a Headway Research instrument at 3000-4000 rpm for periods of 40 seconds

Surface Modification

Plasma Modification

The plasma reactor was designed and built in house by Dongrui Fang [15]. A schematic of the plasma apparatus is shown in figure 1. The entire setup consists of the plasma reactor, rf power generator and matching network, mechanical pump and traps, and gas flow and pressure controllers.

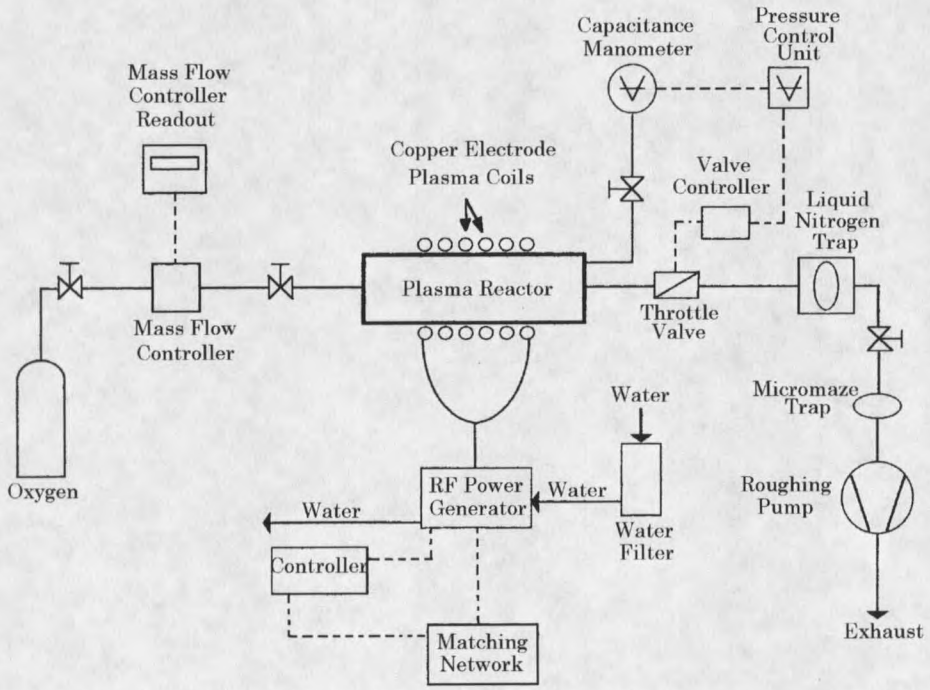

Figure 1. Plasma apparatus

The plasma chamber is composed of a Pyrex glass cylinder that is 24.1 inches long and has an inside diameter of 4 inches and an outside diameter of 4.6 inches. Stainless steel Kurt J. Lester ASA flanges, along with hand cut rubber gaskets, seal each end of the reactor. One flange has two gas feeds and a port for pressure gauges (KJL-205). The other flange has two ports connected to a pressure transducer (Baratron MKS 127A001D) and a pumping line. The flanges are held onto the Pyrex cylinder by four equally spaced bolts that squeeze the cylinder and gaskets between the flanges.

The rf power generator (RF-5S) and matching network (AM-5) are from RF Power Products Inc. The matching network is used to match the impedance of the power amplifier to that of the plasma reactor and is water-cooled. The plasma coil is composed of ¼ inch copper tubing which is wrapped in eight coils around the reactor. The power amplifier is microprocessor controlled with simple push-button operation and digital readouts. It is self-protected with automatic shutdown for high-reflected power, under/over voltage, and excessive temperature. The power amplifier can provide up to 500 Watts output power at 13.56 MHz.

The reactor pressure is measured by an MKS PDRC1C power supply with digital readout that reads the pressure from the pressure transducer (Baratron MKS 127A001D). The reactor pressure is automatically regulated by a MKS throttle valve (MKS 253A220401) that is controlled and powered by a MKS type 152 exhaust valve controller. Gas flow into the reactor is

controlled by a mass flow controller (MKS 1259050SV), a four channel readout and power supply, and shutoff valves (Kurt J. Lester SS-4BKT). This system controls two gas feed lines into the reactor.

The vacuum pump used in this system is a mechanical dual stage pump (Leybold LH-91245-1) with a pumping speed of 4 m^3/hr and can achieve pressures of 10^{-4} torr under ideal conditions. The pumping line has a micromaze trap (Kurt J. Lester MMA-077-2QF), a shutoff valve, and a liquid nitrogen trap. The trap was not used during this study.

Prepared polystyrene samples were placed flat, six at a time, on a horizontal sample tray inside the plasma chamber in the middle of the reactor coil. The chamber was then evacuated for approximately 20 minutes until a vacuum of about 30 mtorr was reached. Oxygen gas was then introduced and allowed to stabilize at a flow rate of 5 sccm at a pressure of 300 mtorr. The rf power amplifier was then turned on to generate the plasma for a period of two minutes. Exposures were made at 20, 100, and 180 Watts rf power. The chamber was then vented to air and the samples were placed in Fluoroware® sample containers.

Molecular Beam Modification

Pulsed beams of energetic oxygen atoms are produced with a laser detonation source [17], which is coupled to a crossed molecular beams apparatus [18,19] for beam diagnostics [20]. A rotatable quadrupole mass

spectrometer is placed in line with the source for beam characterization. Figure 2 shows a schematic diagram of the apparatus. A pulsed CO_2 laser is used to induce a high temperature plasma in a "slug" of O_2 gas that is injected with a pulsed valve into the confined region of a conical nozzle. As a result of efficient electron-ion recombination in the rapidly expanding plasma, an expanding cone of essentially neutral species with hyperthermal velocities is produced.

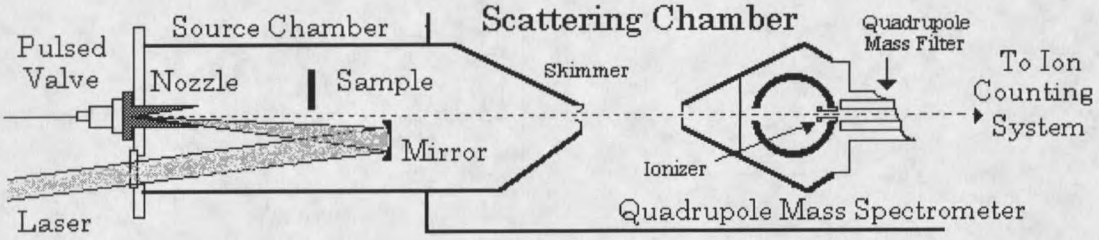

Figure 2. Neutral molecular beam source

A typical pulse contains a mix of atomic and molecular oxygen in a ratio of approximately 60/40, respectively, traveling at an average velocity of about 8 km/s (5 eV of kinetic energy for O atoms). The O/O_2 ratio and the nominal beam velocity can be varied over a wide range by adjusting the valve operating voltage, the time the valve is open, the pressure of the gas behind the valve, the laser power, and the delay in firing the laser.

The source chamber is pumped by a ten-inch oil diffusion pump backed by a Welch Duo-Seal mechanical pump. The laser is an Alltec Al-851 commercial CO_2 laser. An Edwards thermocouple gauge (AIM-S-NW25) and controller (ADG) and a Dunway Stockroom Corp. ion gauge (I-075-N) with a

Granville-Phillips controller are used to monitor pressure. The quadrupole mass spectrometer is from Extranuclear Laboratories. The ion counting system and ionizer are home built and are described in detail in reference [18], and uses a quad discriminator (Leroy 821), log/ln rate meter (Ortec 449), and a PC-mounted multi-channel scaler (EG&G Ortec ACE-MCS).

Prepared polystyrene samples were placed in a sample holder that holds nine samples. The holder was then placed to hold the samples perpendicular to the beam axis at a distance of 31.4 cm from the apex of the source's conical nozzle, see figure 7. The source chamber was then evacuated to a pressure of 10^{-6} torr. The oxygen feed gas to the pulsed valve was set at 125 psig. The pulsed valve was set to operate with 800 volts and a 100 μsec. wide pulse. The pulsed valve is triggered at $t = 0$. The CO_2 laser was set to fire 245 μsec. after the pulse valve was triggered. The laser was producing 5.5 joules/pulse. The laser and pulsed valve were operated at a frequency of 1.8 Hz, resulting in an atomic oxygen flux at this distance of approximately one monolayer per second (10^{15} atoms/cm^2/s). The time of flight and kinetic energy distributions of the molecular beam used to expose the samples in this study are shown in figure 3. The beam was composed of 59% oxygen atoms with an average kinetic energy of 4.6 eV and 41% oxygen molecules with an average kinetic energy of 9.8 eV. Samples were exposed to durations of 10, 100, 500, 1000, and 10,000 total pulses. The chamber was vented to air and the samples were removed and placed in Fluoroware® sample containers.

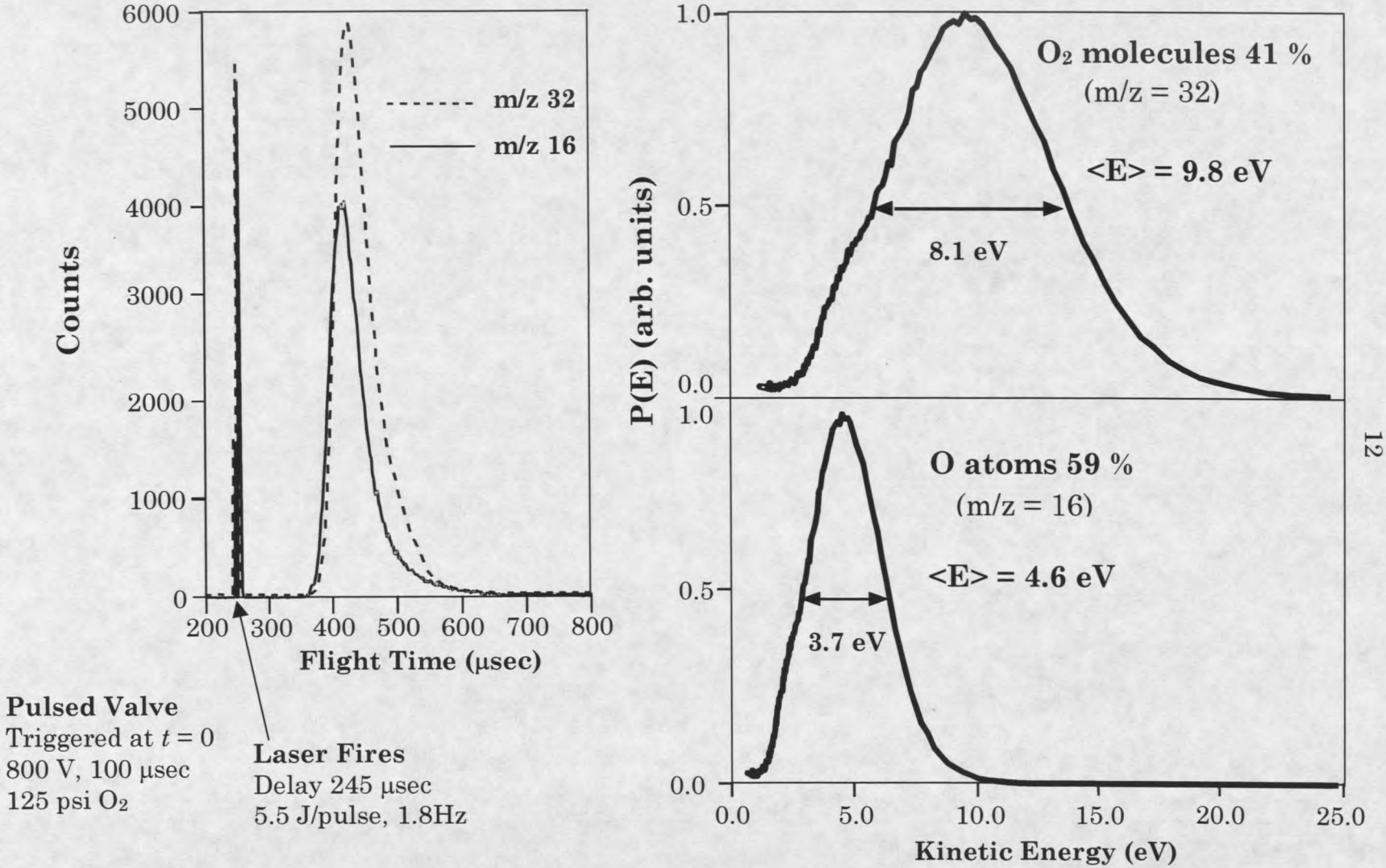

Figure 3. Time-of-flight and kinetic energy distribution of molecular beam

Analytical Techniques

X-ray Photoelectron Spectroscopy

X-ray Photoelectron Spectroscopy (XPS), also commonly called Electron Spectroscopy for Chemical Analysis (ESCA), is the primary analytical technique used to determine polymer surface composition and structure in this study. This technique offers several advantages for analyzing polymer surfaces. XPS is relatively nondestructive of the sample being analyzed. It can detect all elements except hydrogen and helium with good sensitivity (parts per 1000). It provides quantitative elemental composition. It is surface sensitive, analyzing the top 1 to 10 nanometers of the surface. It can provide chemical bonding information such as oxidation states and bonding atoms. XPS has the disadvantages of fairly low resolution, slow analysis time, and requires a large analysis area. On non-conducting samples, charging and energy reference problems can arise. XPS requires high vacuums of 10^{-9} torr, so the sample being analyzed must be stable at these pressures and not outgas significantly. XPS is also very expensive. Sample analysis runs $50 to $500 per sample, while the instruments can cost as much as $500,000 [12].

The photoelectric effect is the basic principle of x-ray photoelectron spectroscopy. When a photon interacts with matter, a number of things can happen. The photon may pass though the atom without interacting with the

nucleus or any of the orbital electrons. The photon may be deflected by an orbital electron and lose some of its energy, this is called Compton scattering. The last thing that may occur is that the photon may interact with a core level atomic orbital electron in such a way that the electron absorbs the entire energy of the photon. If the photon energy, $h\nu$, is greater than the electron binding energy, E_b, the electron will be ejected with a kinetic energy E_k. If the kinetic energy of the ejected electron is measured and we know the energy of the photon, the electron binding energy can be calculated. In gasses, the binding energy is equal to the ionization energy of the electron, but for solids the influence of the surface is felt and additional energy is required to remove the electron from the surface. This additional energy is called the work function (ϕ). Figure 4 shows a diagram of the photoelectric effect and the equation for calculating the electron binding energy [13].

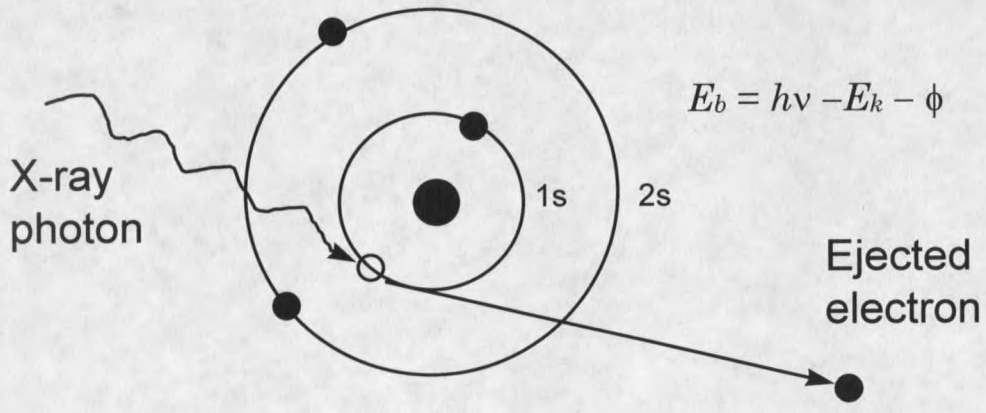

Figure 4. The photoelectric effect

The binding energy of an electron is specific to the element it came from and its bonding environment. The number of emitted electrons for a given atom is proportional to the concentration of that atom in the sample. By measuring the number of emitted electrons and their energies, the element and its concentration can be determined.

Energy referencing and sample charging need to be addressed. As electrons are emitted, the sample develops a positive charge. Conducting samples are grounded to the spectrometer, and do not develop a positive charge as electrons are ejected from the sample. Insulating samples, on the other hand, do develop a positive charge as electrons are ejected. This positive charge acts as an electrical potential barrier that must be overcome by photoelectrons leaving the surface. Hence, the electron loses some energy and appears in the XPS spectrum at a higher binding energy than it would if charging had not occurred. This apparent binding energy shift depends upon the particular instrument, the sample type and its dimensions and mounting method [12]. The charging effects are handled in modern instruments with a low energy (<20 eV) electron gun, which floods the surface with an electron cloud to replace the emitted electrons. Because of instrumental and sample variations, it is difficult to achieve an absolute energy reference scale. In this case, a reference photoionization peak is chosen and the peaks are referenced to this peak. The entire spectrum is shifted the same amount as the reference peak. This works very well if the instrument is properly calibrated

[12]. In the case of organic polymers, the reference peak is usually the saturated hydrocarbon carbon 1s orbital electron peak. This peak is conventionally reported in the literature as occurring at 285 eV. In most of the spectra in this study, the carbon 1s (C1s) peak actually occurred anywhere from 282 eV to 285 eV. All spectra in this study are numerically shifted so the C1s peak occurs at 285 eV.

A basic schematic of a modern XPS instrument very similar to the one that was used for these studies is shown in figure 5 [13]. The basic components of an XPS instrument are an x-ray source, ultrahigh vacuum chamber, electron energy analyzer, and data collection and analysis system. A monochromatic x-ray source was used for this study. A heated filament is used to produce electrons. These electrons are then accelerated in an electric field of 15 kilovolts towards an aluminum anode. The high-energy electrons interact with the aluminum to produce a beam of aluminum Kα x-rays with energies of 1486.6 eV. This x-ray beam is dominated by $K\alpha_{1,2}$ x-rays. Additionally, x-rays such as $K\alpha_{3,4}$, Kβ, and others are also produced and are called satellite x-rays. There is also a considerable amount of high-energy broadband x-ray radiation produced commonly called white radiation. By diffracting aluminum Kα x-rays from a spherically curved quartz crystal, a monochromatic beam of $K\alpha_{1,2}$ photons is produced. This results in simpler spectra, lower background, higher resolution, and minimized radiation damage to the sample when compared to using a non-monochromatic source.

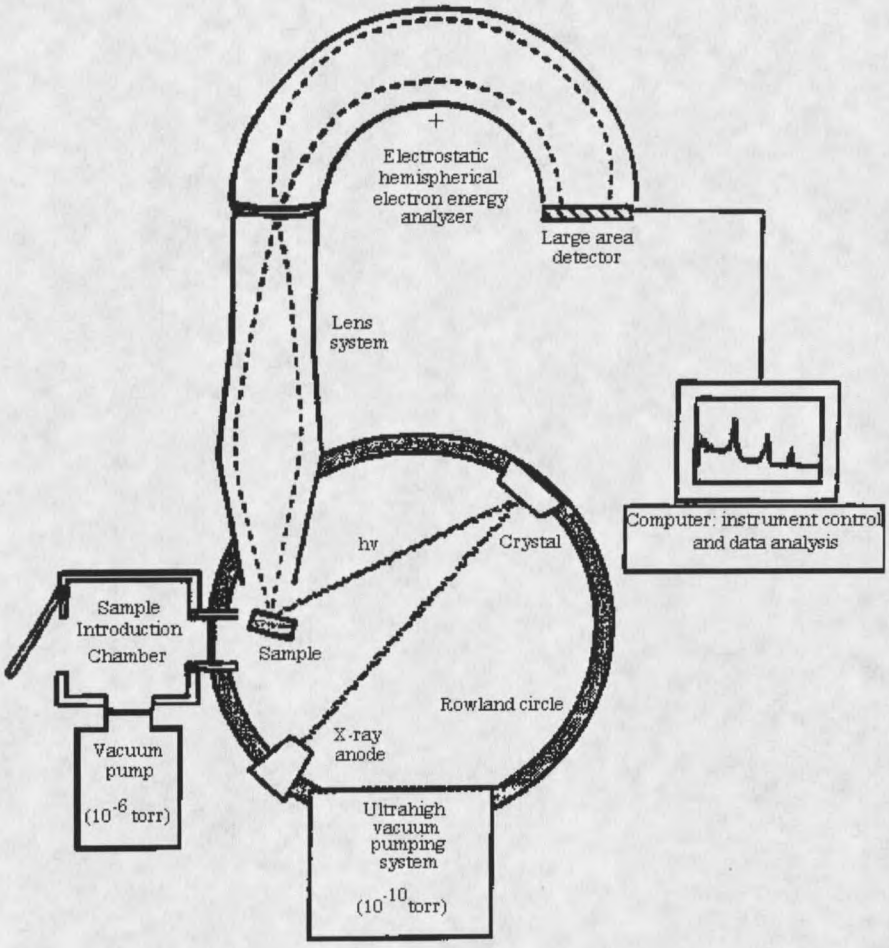

Figure 5. X-ray photoelectron spectrometer

A monochromatic source has the big disadvantage of providing several orders of magnitude less x-ray flux at the sample, requiring greater efficiency in the detection system and a longer analysis time needed for additional signal averaging [12].

An ultrahigh vacuum system is required for three reasons. First, the emitted photoelectrons should not collide with gas particles on their journey

from the sample to the detector. Second, several of the XPS components like the x-ray source only operate in a vacuum. Lastly, the sample should not become contaminated from interactions with atoms and molecules in the residual vacuum during the course of an XPS experiment [13].

The energy analyzing system consists of the lens system, energy analyzer, and detector. The electrostatic hemispherical electron energy analyzer consists of two concentric hemispheres. A voltage difference is placed across the two hemispheres so that the outer one is negative and the inner one is positive. This voltage difference is fixed during the course of an analysis run to allow electrons of only one kinetic energy entering the analyzer to pass though to the detector. This is known as operating in a constant resolution mode, meaning that all the photoionization peaks of a sample will have the same peak width. The energy an electron requires to pass though the analyzer is called the pass energy. High-resolution spectra typically have pass energies of 5 to 25 eV, while low-resolution spectra have pass energies of 100 to 200 eV [13]. The lens system collects the electrons from the sample and operates to retard the kinetic energies of the electrons leaving the sample to the pass energy of the electrostatic hemispherical electron energy analyzer. The pre-retardation voltages in the lens system are varied to scan the kinetic energy range of interest. A multichannel detector counts the number of electrons hitting it and passes the count to the computer control system. The computer control system provides for control of

the pass energies, lens system, and x-ray source. It also provides for data collection, storage, and analysis.

Figures 6 and 7 show the two types of spectra that are commonly seen. The spectra are both generated from poly(vinyl alcohol). The x-axis is electron binding energy in electron volts, and the y-axis is related to the number of electrons that are detected. One, shown in figure 3, is called a survey spectrum, where an entire energy range, usually 0 to 1200 eV, is scanned. The 1200 eV range is chosen because all the detectable elements have photoionization peaks that occur within that range.

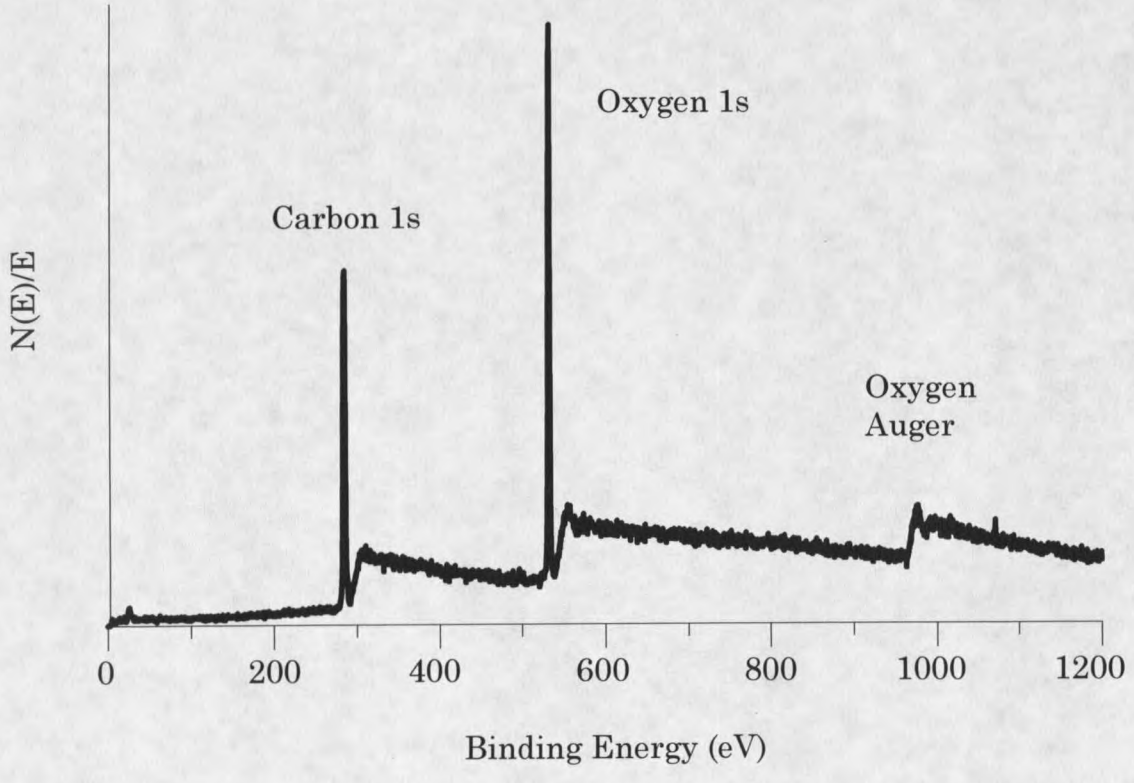

Figure 6. Survey spectrum of poly(vinyl alcohol)

There are a number of features to note about this spectrum. First, there are the two photoionization peaks at 285 and 540 eV. The peak intensity and area are proportional to the amount of the element once the consideration has been taken into account that different elements and different orbital electrons have different photoionization cross-sections. In other words, different elements have different probabilities that core level electrons will be emitted. Another feature to note is the step pattern of increasing baseline after each peak. The x-ray photons penetrate a considerable depth into the sample and cause electron emission throughout the sample. Only those electrons that are close enough to the surface escape without losing energy by inelastically scattering off other atoms will contribute to the photoionization peak. Electrons from the surface that have lost energy contribute to the inelastic scattering tail that occurs after each peak. The remaining feature at 970 eV is an oxygen Auger peak. An Auger electron occurs when a photoionized atom becomes de-excited through a non-radiative process. An inner higher energy orbital vacancy is filled by an outer lower energy orbital electron from the same atom causing an electron to be emitted carrying off the extra energy. The spectral features in the 0 to 30 eV range are from photoionization of weakly bound electrons in valence shells and molecular orbitals and have been used in the study of polymers using XPS [14].

The spectrum in figure 7 is an example of a high-resolution scan. Such scans are performed at a higher energy resolution on a narrow energy range

around each of the elements of interest that were determined from the survey scan. The survey spectra in this study had a resolution of 0.25 eV and the high-resolution spectra had a resolution of 0.1 eV. The range for the carbon 1s peak is 280 eV to 295 eV. The feature of interest in this spectrum is the carbon 1s peak being made up of multiple peaks due to having some of the carbons being bound to oxygen in the polymer. Atomic concentrations and chemical bonding information are determined from high-resolution scans in this study.

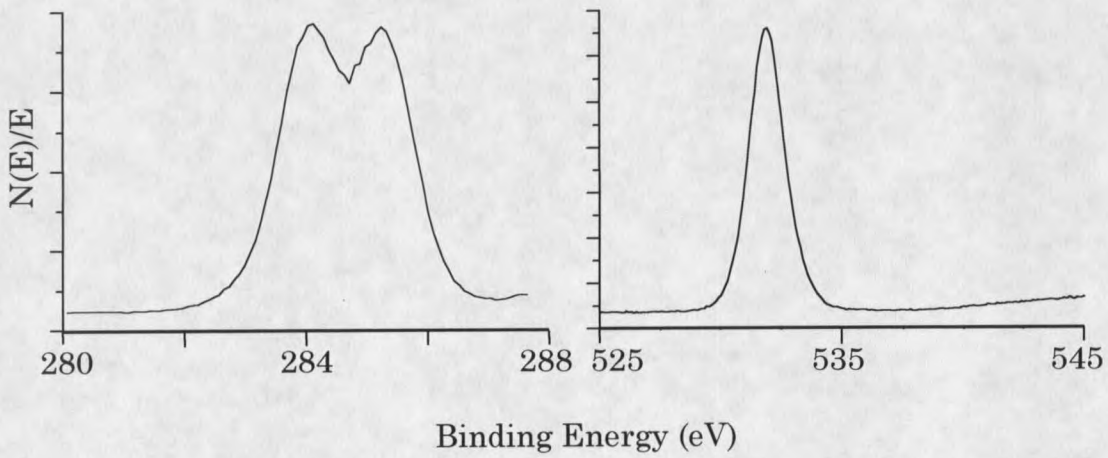

Figure 7. High resolution spectrum of poly(vinyl alcohol)

XPS spectra were collected with a Physical Electronics (PHI) model 5600CI spectrometer. The instrument is located at the Image and Chemical Analysis Laboratory (ICAL), Montana State University-Bozeman. An aluminum monochromatic 7mm source operating at 300 Watts was used for

the x-ray source. The x-ray source provided monochromatic $K\alpha_{1,2}$ photons that have an energy of 1486.6 eV. The energy analysis system was used with an aperture setting of 4 which corresponds to an analysis spot size of 800 μm. The main chamber was maintained at 10^{-9} torr, while the introduction chamber was maintained at 10^{-7} torr. Because polystyrene is nonconductive, the electron flood gun for charge compensation was operated at a value of 21.5 with electron energies of 5 to 11 %. Survey spectra were obtained with a pass energy of 93.900 eV. High-resolution spectra used a pass energy of 23.500 eV. The x-ray source and energy analyzer aperture were both at 45 degrees from normal to the surface for all analyses.

C1s Curve Deconvolution in XPS Spectra

Carbon 1s electrons have binding energies of ~285 eV in a saturated hydrocarbon. This binding energy can change when the carbon is in different bonding environments. This is especially true when carbon atoms are bound to electronegative atoms such as oxygen and fluorine. Hence, a carbon atom in an ether environment can be differentiated from a carbon atom in a carboxylic acid environment. However, peaks that are separated by less than one eV often can not be resolved with any detail by XPS. In these cases, mathematical curve deconvolution is used to resolve peaks that are too close together. Chemical binding energy shifts for carbon containing molecules are generally referenced to the saturated hydrocarbon peak at 285 eV. Hence, a

carbon atom in a carboxylic acid having a peak at 289 eV is listed as having a chemical shift of 4 eV. Tables 1, 2, and 3 list the binding energies for various functional groups that are of importance to this study. These tables were adapted from appendices 1 and 2 in reference 14. Primary C1s chemical shifts are defined as when the chemical shift of a carbon is the result of the carbon being directly bound to the heteroatom causing the shift. Secondary C1s chemical shifts result when the carbon being shifted is bound to another carbon that is bound to the heteroatom causing the chemical shift. In Tables 1, 2, and 3 the carbon whose shift is being looked at is denoted by underlining. The curve deconvolution is done on the C1s spectrum of the sample being analyzed. The C1s peak is fit using curves to correspond to the different functional groups so that they add up to the original curve. Fitting is done with a fixed FWHM for all functional groups in a particular sample. The line width for an individual sample can vary somewhat between samples due to differential charging effects [14]. The area under each curve is proportional to the concentration of the corresponding functional group. In this way, the proportions of functional groups present can be quantified to some degree. A concern with this method is that several of the functional group binding energy shifts overlap.

Functional Group	Chemical Shift (eV) Min.	Max.	Mean	Number of Examples
C-O-C	1.13	1.75	1.45	18
C-OH	1.47	1.73	1.55	5
C-O-C=O	1.12	1.98	1.64	21
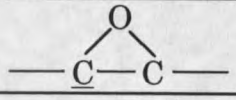			2.02	1
C=O	2.81	2.97	2.90	3
O-C-O	2.83	3.06	2.93	5
C-O-C=O	3.64	4.23	3.99	21
O=C-OH	4.18	4.33	4.26	2
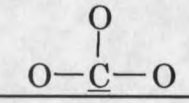	4.30	4.34	4.32	2
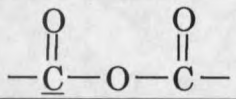	4.36	4.46	4.41	3
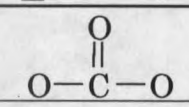	5.35	5.44	5.40	2

Table 1. Primary C1s chemical shifts with oxygen [14]

Functional Group	Chemical Shift (eV) Min.	Max.	Mean	Number of Examples
C-Cl	2.00	2.03	2.02	2
CF_3	7.65	7.72	7.69	2
C=C	-0.24	-0.31	-0.27	4
C-Si	-0.61	-0.78	-0.67	3
N-C=O	2.97	3.59	3.11	6
N-C-O			2.78	1
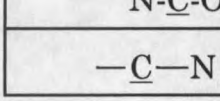	0.56	1.41	0.94	9

Table 2. Primary C1s chemical shifts with atoms other than oxygen [14]

Functional Group	Chemical Shift (eV)	Number of Examples
<u>C</u>-C-O	~0.2	6
<u>C</u>-C-F	~0.4	11
<u>C</u>-C-Cl	~0.5	9
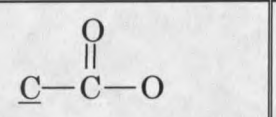	~0.4	7
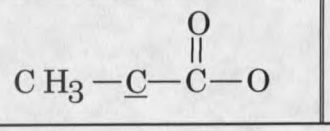	~0.7	8

Table 3 Reference secondary C1s chemical shifts [14]

Accurate curve deconvolution presents a number of problems. First, a number of functionalities overlap in binding energy. Second, a specific functionality can occur over a range of up to one eV when it occurs in different chemical structures. Lastly, it is rather simple to perfectly curve fit a spectrum, but rather more difficult to say that a fitted peak corresponds to something real on a surface that has a variety of functionalities in low concentrations. Most of the literature that uses this technique for assigning functionalities in oxidized polymers assigns the peaks in a straightforward manner [5,7,8,9,10,12,13,14]. The peaks are assigned in the following order: a carbon singly bound to an oxygen at ~1.6 eV, a carbon singly bound to two oxygens or doubly bound to one oxygen at ~3 eV, a carbon singly bound to one oxygen and doubly bound to another oxygen at ~4 eV, and finally a carbon singly bound to two oxygens and doubly bound to another oxygen at ~ 5.4 eV.

The secondary C1s chemical shift designated as C-CO_2 or β-CO_2 is also assigned at ~0.6 eV and is fit with the same area as the carboxyl group. Peak fitting the beam modified sample spectra in this simple manner provided nonsensical results. Few of the literature references have binding energy shifts for epoxides [14,21]. These references, along with the epoxide data from this study, support a value of 2 eV for the chemical shift for an epoxide. The shape of the C1s spectra of the beam modified PS samples and the derivatization results, support fitting a peak at 2 eV. The exact chemical nature of this peak is undetermined at this time although the peak is labeled as an epoxide. The carbon singly bound to an oxygen in the C-O-CO-C group had values from 1 to 2 eV [14]. Ethers have values of 1 to 1.75 eV, and alcohols ranged from 1.5 to 1.7 eV [14]. The best curve fits were achieved by fitting the C-O peak towards the 1 eV value. The exact chemical nature of the peak at ~5 eV is also undetermined at this time even though the literature label C-O peaks in this area as carbonates.

The beam modified spectra were fit with the β-CO_2 at 0.6 eV, the carbon singly bound to a oxygen at ~1.0 eV, a so called epoxide peak at 2.0 eV, a carbon singly bound to two oxygens or doubly bound to one oxygen at ~3 eV, a carbon singly bound to one oxygen and doubly bound to another oxygen at ~4 eV, and finally a carbon singly bound to two oxygen's and doubly bound to another oxygen at ~ 5.4 eV. The carboxylic acid peak was constrained to have the same area as the β-CO_2 peak. The plasma modified C1s spectra

were fit with the same parameters to provide a direct comparison of the beam and plasma modified spectra even though none of the literature on plasma or photo-oxidized polystyrene perform curve fits with a peak at 2.0 eV. The plasma spectra fit very well with this fitting scheme.

Gaussian fits were performed on each spectrum with a fixed FWHM for all peaks except the $\pi \rightarrow \pi^*$ shakeup satellite. Due to charging effects, the FWHM varied a little from sample to sample, averaging 1.2 for the carbon-oxygen peaks and 1.5 for the shakeup satellite.

Surface Derivatization

Surface derivatization was used in this study to label or tag a particular functional group with an atom that wasn't originally there. The concentration of this new atom can be detected by XPS. The concentration of the original functional group can then be calculated. The literature derivatization reactions that were used are shown in figure 8 [21,22]. These reactions test for hydroxyls, epoxides, carbonyls, and carboxylic acids. Derivatization reactions were performed on modified polystyrene samples and on the reference polymers. Samples were devivatized as shown in figure 9. Samples to be derivatized were suspended in 20-ml borosilicate scintillation vials while reagents were injected into the bottom of the vial so that the samples were not exposed to liquid reagent and only reagent vapor would reach the sample.

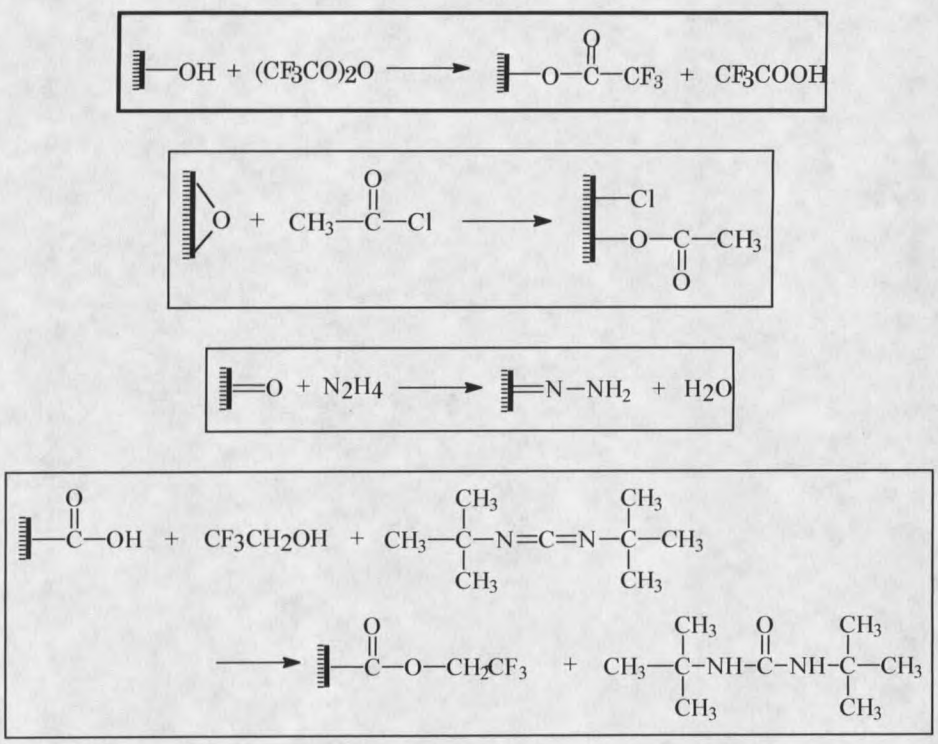

Figure 8. Derivatization reactions

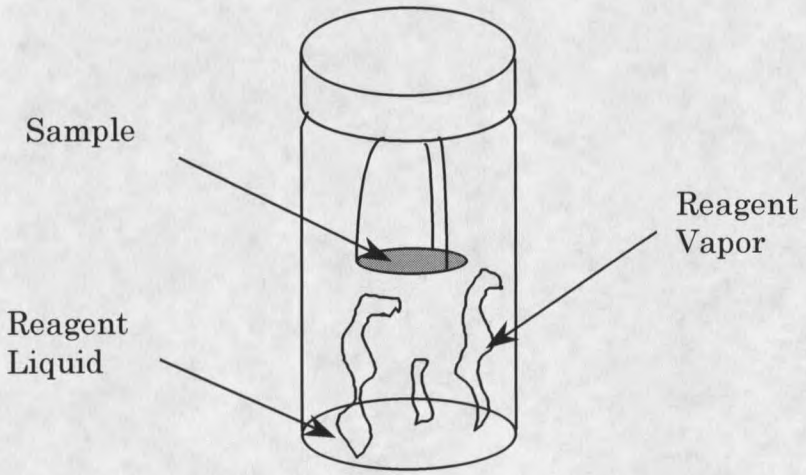

Figure 9. Derivatization reaction vial

The vials were then sealed at ambient pressure with a polypropylene-lined cap. Initial reaction guidelines for the trifluoroacetic anhydride,

trifluoroethanol, and hydrazine reactions were taken from reference 22. Initial acetyl chloride reaction parameters were taken from reference 21.

Trifluoroacetic anhydride (TFAA) (99+%, Aldrich) was used to derivatize hydroxyl functional groups with fluorine. 1 ml of TFAA was placed in the vial. The vial was heated to 50°C in an incubator. The TFAA reaction was allowed to proceed for 60 minutes.

Acetyl chloride (AcCl) (99+%, Aldrich) was used to derivatize epoxide groups with chlorine. 1 ml was placed in the vial, the sample was added, the vial capped, and the reaction was allowed to proceed at ambient temperature and pressure for 5 minutes.

Hydrazine (Sigma Chemical Co., St. Louis, MO) was used to derivatize carbonyl groups with nitrogen atoms. 2 ml was placed in the vial, the sample was added, and the vial was capped. The reaction was allowed to proceed at ambient temperature and pressure for 5 minutes.

2,2,2-Trifluororethanol (TFE) (99+%, Aldrich), along with 1,3-Di-*tert*-butyl carbodiimide (Di-tBuC) (99%, Aldrich), and pyridine (99+%, Sigma), were used to label carboxyl groups with fluorine. TFE (0.9 ml), pyridine (0.4 ml), and Di-tBuC (0.3 ml) were added sequentially to the vial every 15 minutes. When all reagents were added, the reaction was allowed to proceed for approximately 12 hours at ambient temperature and pressure.

Functional group percentage on the surface requires calculation from the atomic concentration of the labeling atom. If the assumption that the

reaction is selective, stoichiometric, and goes to completion is followed, a simple calculation can be used to determine the percent functional group on the surface as given in figure 10.

$$\% \text{ Functional Group} = \frac{\%T}{N_T\,[100 - \%T(N_A/N_T]} \quad X\ 100$$

Figure 10. Percent functional group calculation

% FG is defined as [moles of functional group/total surface moles] X 100. % T is the atomic concentration of the labeling atom as determined by XPS. N_T is the number of tag atoms added for each functional group. N_A is the net change in the number of atoms during the reaction for each functional group [4]. For the hydroxyl reaction, three fluorine tag atoms are added for each functional group so N_T is equal to three. The original functional group contained one oxygen atom and the derivatized functional group contains two oxygen, two carbon, and three fluorine molecules, so N_A is equal to seven minus one for a value of six. Recall that hydrogen is not detected by XPS so hydrogen molecules are not factored into the calculation. This method assumes an ideal surface derivatization reaction is being used. This method was originally developed for looking at just hydroxyl concentrations and requires a slight adjustment when looking at mixed systems. It works as written for functional groups containing one oxygen atom, where the sum of

the % functional group calculations will add up to the value obtained for the total atomic oxygen concentration in an ideal system. When there are multiple oxygen atoms in a functional group, like a carboxylic acid, the value calculated from the equation needs to be multiplied by the number of oxygen atoms that are in the functional group when making comparisons to the total atomic oxygen concentration.

Scanning Electron Microscopy

Scanning Electron Microscopy (SEM) is a technique used in this study to look at surface topography. The technique can give a magnification of 100,000x with a spatial resolution of 10 nm, one hundred times better than optical microscopes. SEM's also have much greater depth of field than optical microscopes. The technique requires conducting samples. Nonconducting samples can be used if they are coated with a thin coat of gold or carbon. The samples also must be stable under high vacuum.

In SEM the sample is irradiated with a focused, energetically well defined electron beam that is rastered across the sample being analyzed. Many types of signals are produced that give a lot of information about the sample and are discussed in the reference [15]. The signal of interest is from the electrons that are backscattered from the surface. These electrons are detected and converted into a signal that provides an image of the surface.

Images were obtained with a JEOL electron microscope with a JSM-6100 scanning attachment located at the Image and Chemical Analysis Laboratory (ICAL), Montana State University-Bozeman. The samples were first sputter coated with gold-palladium alloy to prevent surface charging problems. An 8.0 keV primary electron beam energy was used to obtain images with a magnification of 40,000 normal to the surface. The analysis chamber was maintained at 10^{-7} torr.

CHAPTER 3

RESULTS AND ANALYSIS

XPS of Polystyrene Surfaces

Unmodified Polystyrene

Figure 11 shows the XPS survey and C1s high resolution spectra of unmodified polystyrene. The unmodified polystyrene has less than 0.5% oxygen content on the surface.

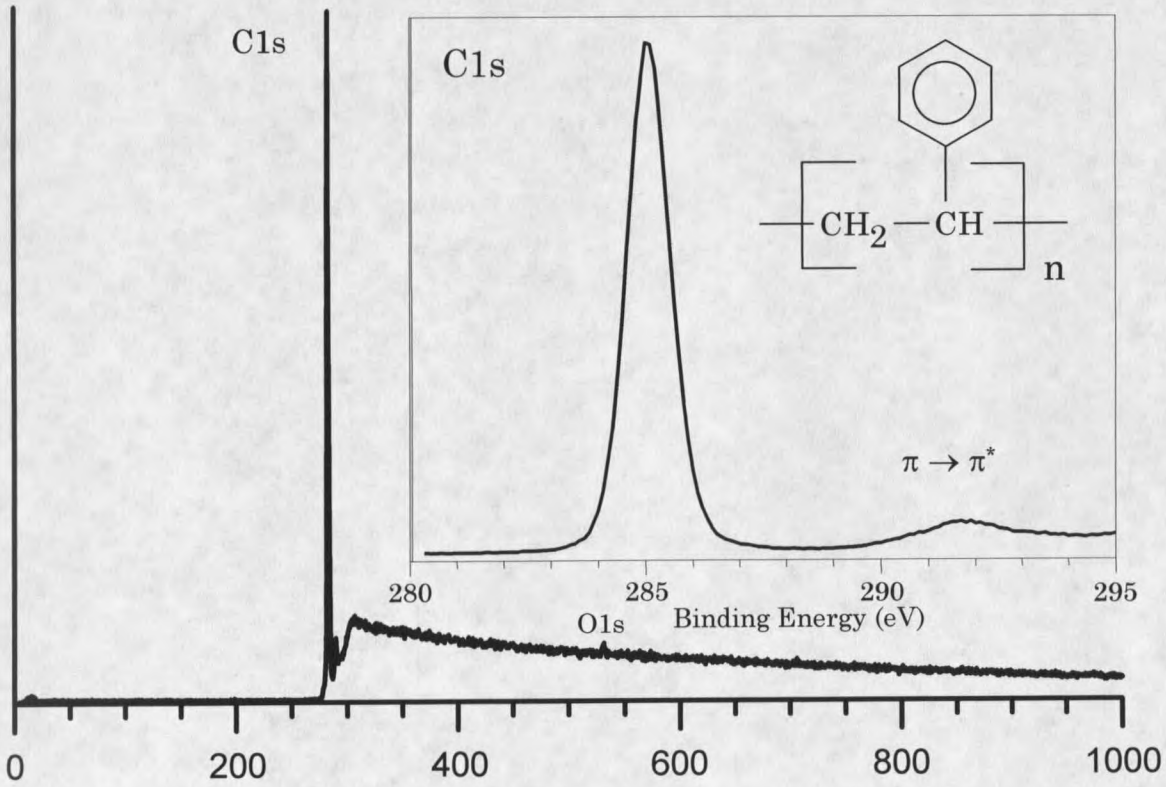

Figure 11. XPS spectra of unmodified polystyrene

There are two important features to note on the C1s spectrum. The main peak at 285 eV is from 1s orbital electrons from the carbon in polystyrene. The peak is narrow and nearly symmetrical. The other feature at 292 eV is called a π to π^* shakeup satellite. This peak occurs when an outgoing photoionized electron loses some of its kinetic energy promoting a valence electron in an occupied orbital (π) to an unoccupied orbital (π^*). Shakeup peaks mostly occur in systems with aromatic character and conjugated double bonds and have been used for quantitative analysis of aromatic polymers [23].

Initial Surface Oxidation

Exposure of polystyrene to oxygen plasmas and hyperthermal oxygen beams results in the incorporation of oxygen into the surface. Table 4 shows the oxygen/carbon ratios on the modified surfaces within days of exposure.

Beam Exposure		**Plasma Exposure**	
Duration (Pulses)	O/C Ratio	Power (Watts)	O/C Ratio
10	0.20	20	0.18
100	0.22	100	0.22
1000	0.24	180	0.25
10000	0.29		

Table 4. Initial atomic concentrations on modified samples

These XPS data show similar oxygen to carbon ratios regardless of exposure conditions, although it appears that the long-duration beam exposure tends to oxidize the surface somewhat more than the most intense plasma treatment. A remarkable observation is that the oxygen atomic concentrations on the beam-treated samples increased by less than 50 percent when the incident atomic oxygen fluence increases by three orders of magnitude. Surface oxidation seems to approach steady state rapidly during the initial attack from the first few monolayers of impinging O atoms. Figure 12 shows an overlay of the C1s spectra of a 10,000 pulse beam sample, 180 W plasma sample, and an unmodified polystyrene sample within two weeks of exposure.

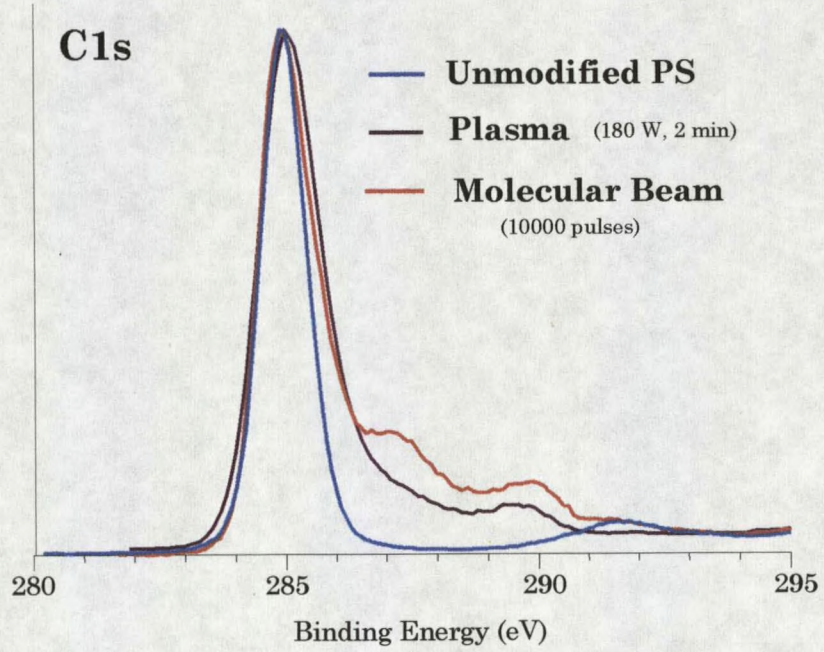

Figure 12. Plasma, beam, and unmodified polystyrene C1s spectra

Both the plasma and beam treated samples exhibit strongly asymmetric peak shapes with higher binding energy components, indicating a wide range of carbon-oxygen bonding environments on the treated surfaces. However, the difference in shape of the curves for the modified surfaces suggests that the distribution of carbon-oxygen bonding environments depends on the exposure method. The depth of the modification may also depend on the exposure environment. The $\pi \rightarrow \pi^*$ shakeup satellite is present in the spectrum of the beam-modified sample and is greatly reduced in the spectrum of the plasma-modified sample. Apparently, the plasma treatment destroys the aromatic character throughout the surface layer probed by XPS. The preservation of aromatic character in the beam treated surface suggests a reduced reactivity of the beam with the aromatic ring. Figure 13 shows the C1s spectra of the 20, 100, and 180 W plasma exposures.

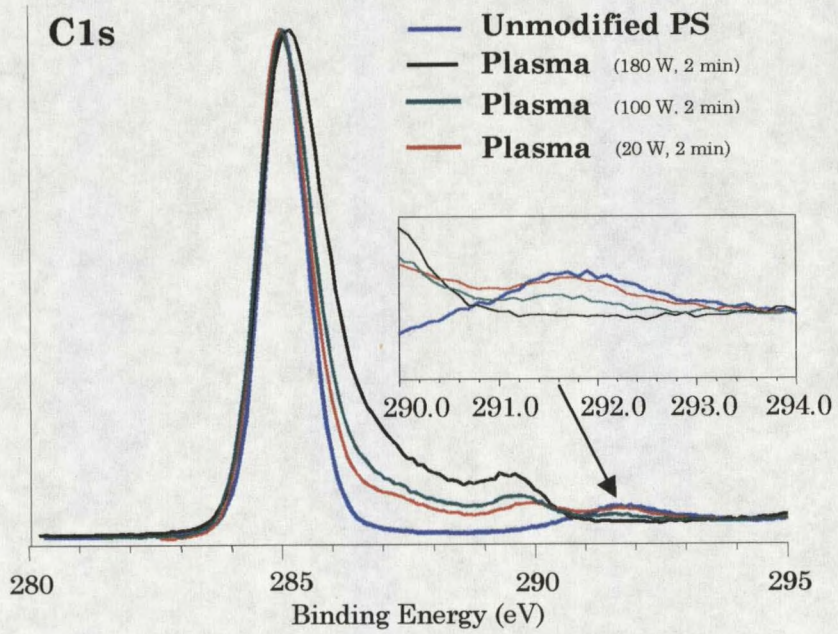

Figure 13. 20, 100, and 180 W plasma modified polystyrene C1s spectra

Figure 14 shows the C1s spectra of the 10, 100, 1000, and 10,000 pulse beam modified surfaces. Notice how similar the 10, 100, and 1000 pulse spectra are to each compared to the 10,000 pulse spectrum.

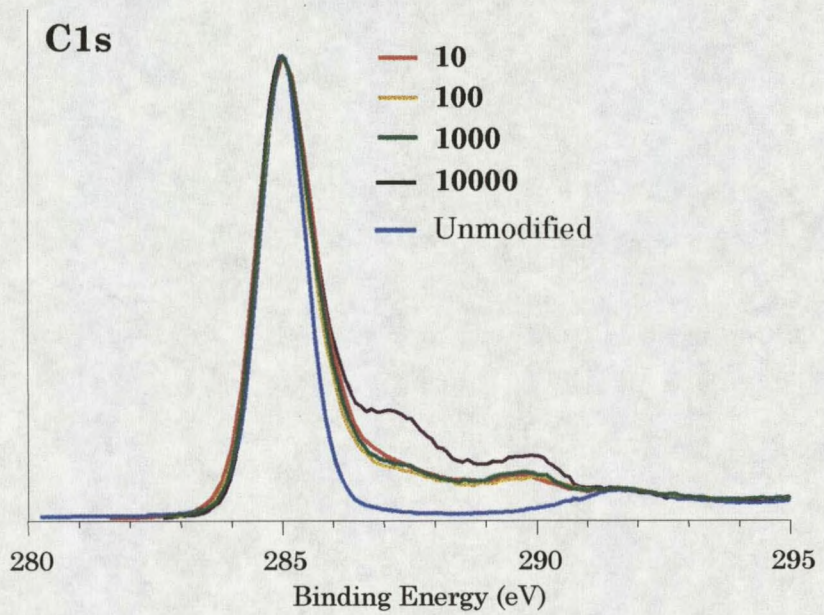

Figure 14. 10, 100, 1000, and 10,000 pulse beam modified PS C1s spectra

This is a very strong indication that a steady state is reached very early on in the surface oxidation process. By the time the 10,000 pulse exposure is completed, significant etching and roughening of the surface has occurred as shown later in this chapter.

Surface Oxidation after One Year

After one year the modified samples were examined again. A significant loss of oxygen occurred on the beam modified samples, especially

the 10,000 pulse beam sample. By exposing another set of 10,000 pulse samples and analyzing them periodically, it was determined that the surface change occurred within two weeks. Table 5 shows the oxygen/carbon ratios for the one year-old samples. Notice that the O/C ratios on the 100, 1000, and 10,000 pulse surfaces changed to become very similar in oxygen content to the 10 pulse surface.

Beam Exposure (1 year)			**Plasma exposure** (1 year)		
Duration (Pulses)	O/C Ratio	Percent Change	Power (Watts)	O/C Ratio	Percent Change
10	0.17	-15	20	0.17	-5.5
100	0.17	-23	100	0.19	-13.6
1000	0.18	-25	180	0.24	-4.0
10,000	0.18	-38			

Table 5. Atomic concentrations on modified samples after one year

Figure 15 shows the C1s spectra from the same 10,000 pulse beam sample one year apart.

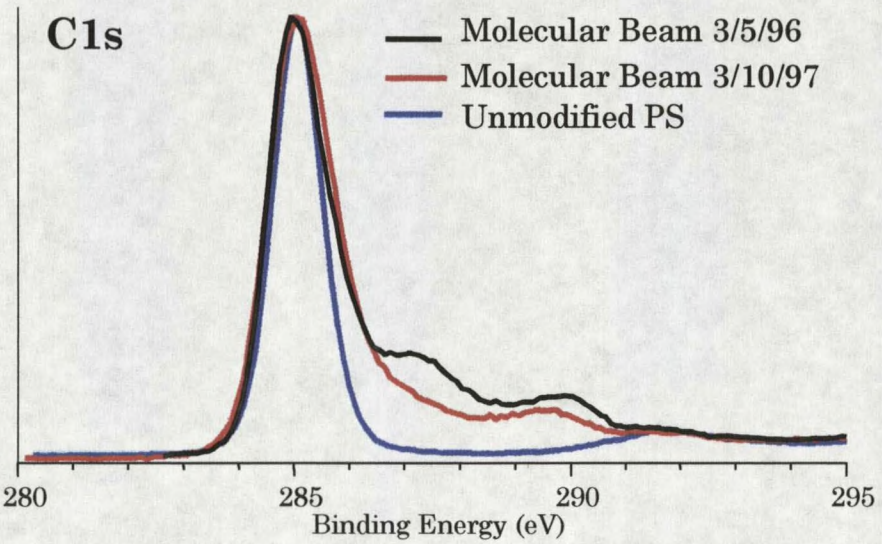

Figure 15. One year 10,000 pulse beam modified polystyrene C1s spectra

The major change in the spectra appears to be centered on the 287 and 290 eV peaks on the fresh surface. By performing C1s curve deconvolution, an attempt was made at identifying the species that are disappearing. Further work is being carried out in the group on directly determining the identity of products that are weakly bound to the oxidized surfaces. By fitting the spectrum with values determined in chapter 2, figures 16 and 17 were obtained. The presence of a substantial amount of epoxide groups on the surface is supported by the derivatization studies.

Figure 18 shows the 10, 100, 1000, and 10,000 pulse beam sample C1s spectra one year after initial exposure. The spectra are nearly identical in carbon-oxygen bonding environments with very similar overall oxygen/carbon ratios. In other words, the different durations of hyperthermal molecular beam exposure become nearly identical in chemistry within two weeks after exposure.

In contrast, when the C1s spectrum of a 180 W plasma modified sample is looked at, the overall change after one year is significantly less than that of the 10,000 pulse beam modified sample. Figure 19 shows the C1s spectra of the same plasma surface initially and after approximately one year. It can be seen that the carbon/oxygen functionality distribution is essentially unchanged even though the peak widths are different due to charging effects.

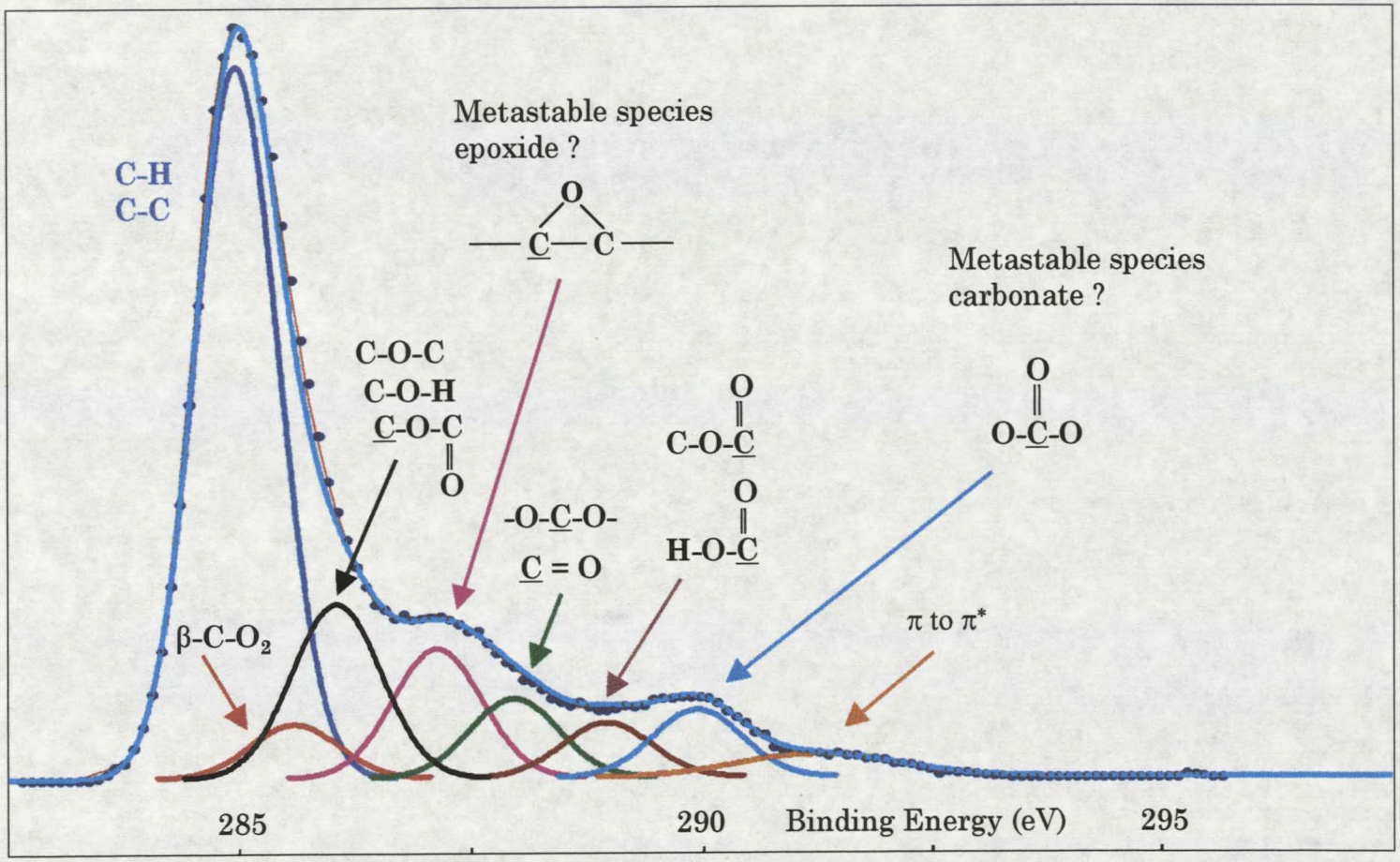

Figure 16. 10,000 pulse beam surface peak-fitting

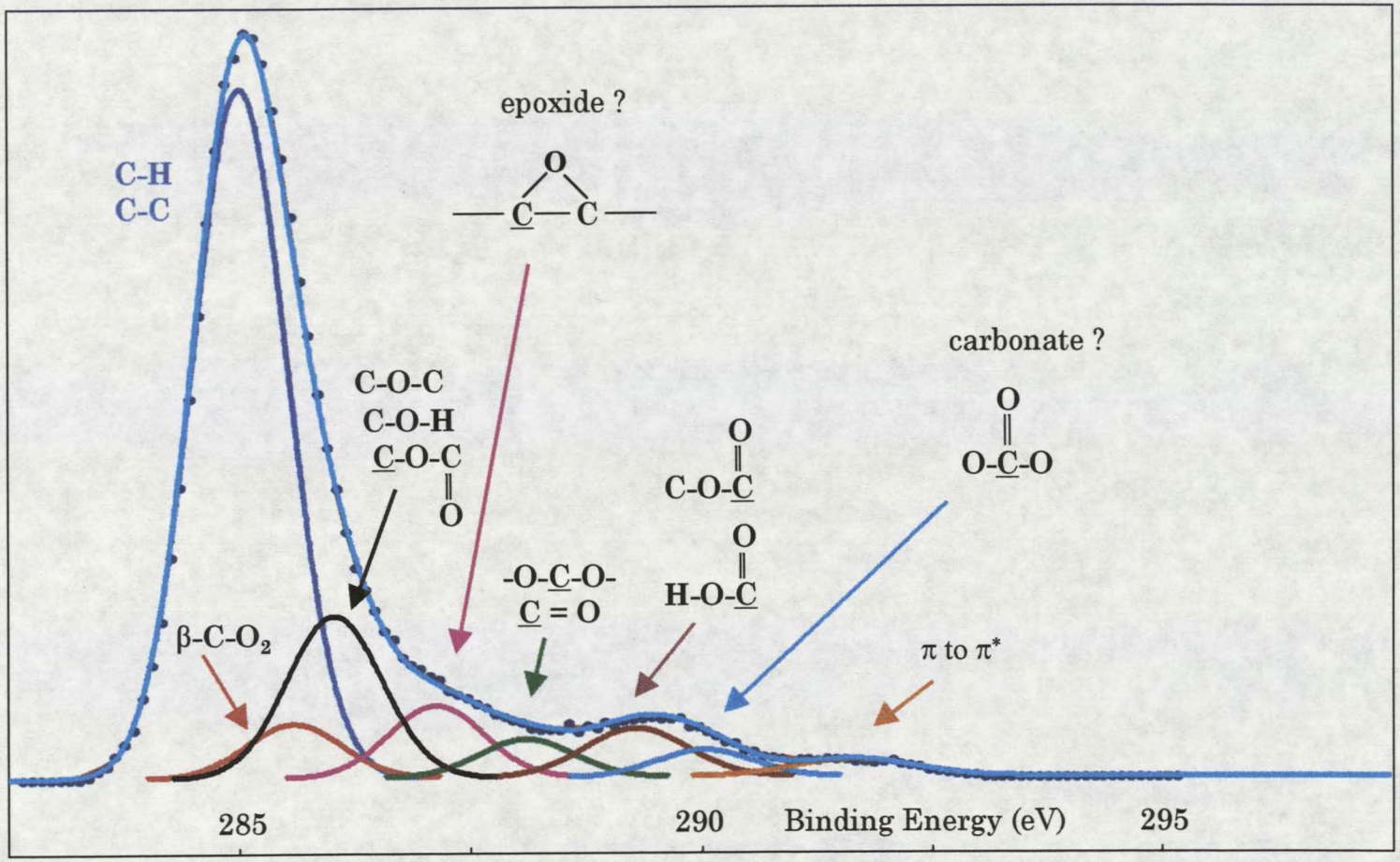

Figure 17. One year-old 10,000 pulse surface curve deconvolution

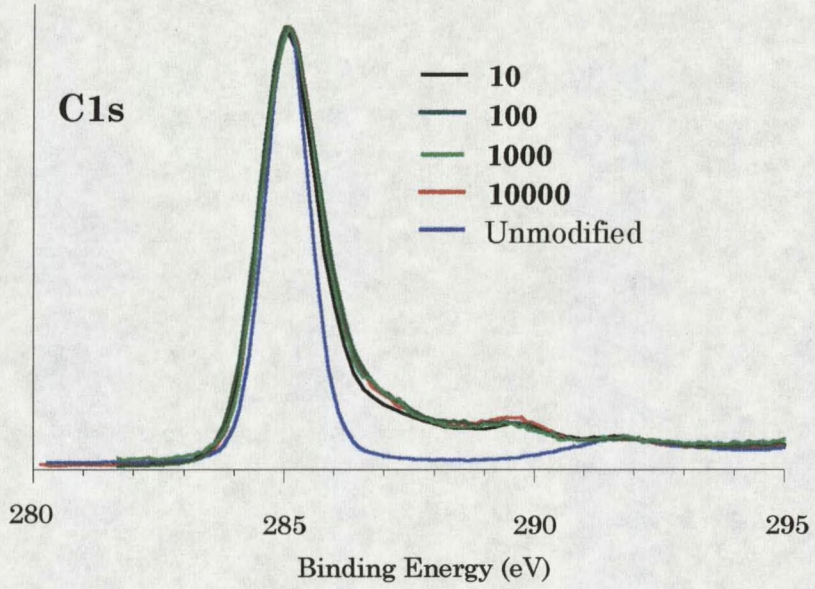

Figure 18. One year-old beam modified polystyrene C1s spectra

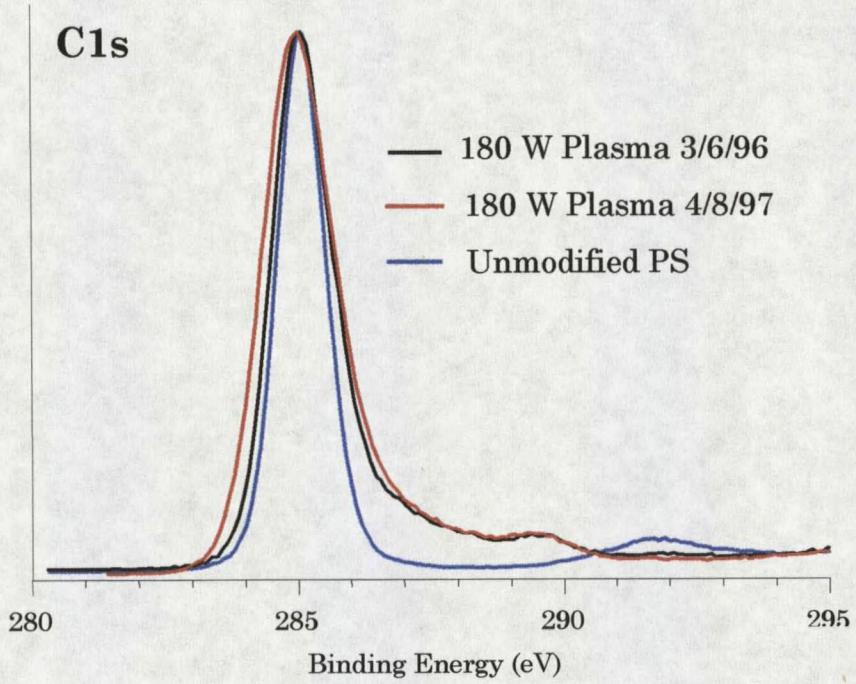

Figure 19. One year plasma modified polystyrene C1s spectra

Tables 6 and 7 summarize the beam and plasma peak fitting data. The β-CO_2 is not regarded as an oxidized species, so it is not used in the functional group calculations. The percent functional groups were calculated by taking the peak area of a peak and calculating its percentage out of the sum of the oxygen functional groups which were constrained to add up to 100%. This value was then multiplied by the total atomic oxygen concentration. The $\pi \rightarrow \pi^*$ satellite is included to show a measure of the loss of aromaticity. The data in tables 6 and 7 support the qualitative observations from the spectral and atomic concentration comparisons. The data show a loss of the aromaticity in the beam exposed surfaces, which is not apparent from looking at the spectra. The beam exposed surfaces show a significant gain of oxygen in proportion to duration of the exposure that occurs most strongly in the epoxide, carbonyl, and carbonate functionalities. The loss of oxygen after one year is also concentrated in the epoxide, carbonyl, and carbonate functionalities. The 10 and 100 pulse beam samples show a loss of acid groups, while the 1000 and 10,000 pulse samples do not. The plasma exposed surfaces show a progressive loss of aromaticity with total loss of the aromatic character in the 180 W sample. The plasma modified surfaces show a slight across the board decrease in oxygen and are essentially unchanged.

Species → Sample ↓	C-H % of C1s	$\pi \rightarrow \pi^*$ % of C1s	% Functional Group of Total Oxygen Atomic Concentration					
			Atomic Concentration of Oxygen	C-O	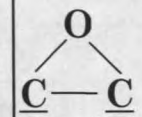	C=O	O-C=O	O-CO-O
Unmodified	95.7	4.3	0.0					
10	68.6	2.3	16.7	6.4	3.7	2.4	2.2	2.0
100	67.1	2.4	18.0	7.1	3.9	2.5	2.3	2.2
1000	63.8	2.8	19.4	8.1	4.0	2.4	2.5	2.4
10,000	52.7	3.2	22.3	7.7	5.7	3.5	2.4	3.0
10 (1 yr)	66.6	2.5	14.5	7.5	3.5	1.6	1.0	0.9
100 (1 yr)	63.2	1.8	14.5	7.3	3.5	1.7	1.1	0.9
1000 (1 yr)	65.8	1.9	15.3	7.4	3.6	1.3	2.2	0.8
10,000 (1 yr)	61.9	1.9	15.3	7.1	3.1	1.6	2.3	1.2

Table 6. Beam modified surface functional group curve deconvolution summary

Species → Sample ↓	C-H % of C1s	$\pi \rightarrow \pi^*$ % of C1s	% Functional Group of Total Oxygen Atomic Concentration					
			Atomic Concentration of Oxygen	C-O	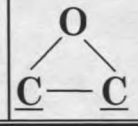	C=O	O-C=O	O-CO-O
Unmodified	95.7	4.3	0.0					
20 W	75.4	3.0	15.3	6.8	3.5	1.6	1.1	2.3
100 W	72.2	1.3	18.0	7.8	4.1	2.4	3.1	0.5
180 W	72.2	0.0	20.0	9.1	4.7	2.8	3.3	0.1
20 W (1 yr)	75.6	2.7	14.5	6.7	3.2	1.6	1.0	1.9
100 W (1 yr)	71.6	0.6	16	7.7	3.8	2.1	2.1	0.3
180 W (1 yr)	70.9	0.0	19.4	9.4	4.6	2.4	2.8	0.2

Table 7. Plasma modified surface functional group curve deconvolution summary

Surface Derivatization

Reference Polymers

Spin cast reference polymers were tested by XPS with C1s curve deconvolution to test their purity and structure. Samples that showed more than 2.0% contamination of were not used for study. There was significant silicon contamination traced to the filters used for filtering the polymer solutions before spin casting. This was most prevalent for the polymers dissolved in organic solvents. In these cases no filtering was done. Poly(epoxy propyl methacrylate) was received in solution and always showed small amounts fluorine and silicon contamination. The reference polymers, each containing one of the functional groups in question, are shown in figures 20 and 21.

Poly(vinyl methyl ketone) PVMK

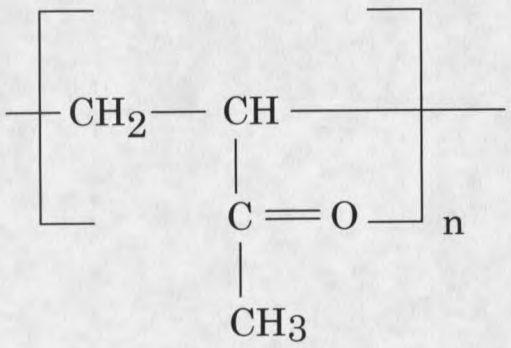

Poly(acrylic acid) PAA

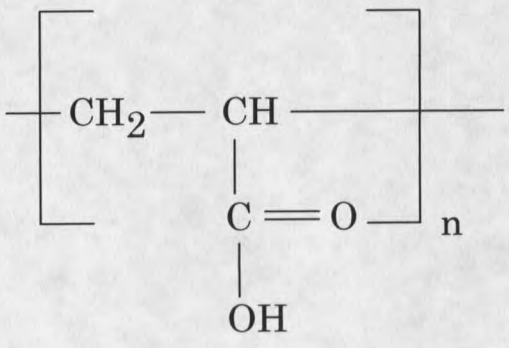

Figure 20. Reference polymer structures

Poly(epoxy propyl methacrylate) PEPMA

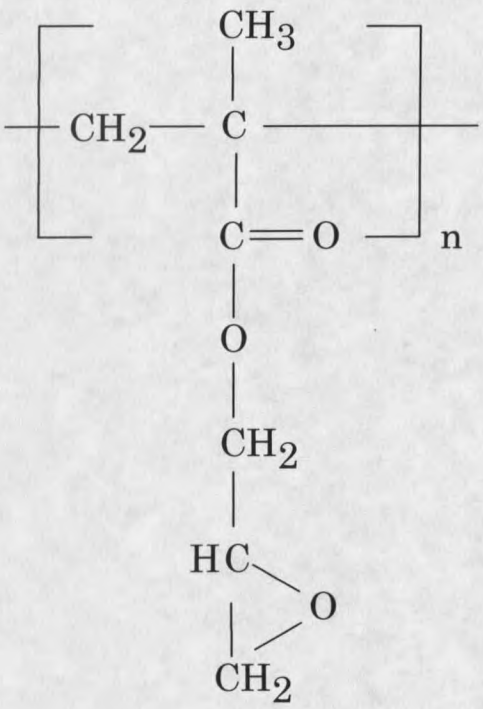

Poly(vinyl Alcohol) PVA

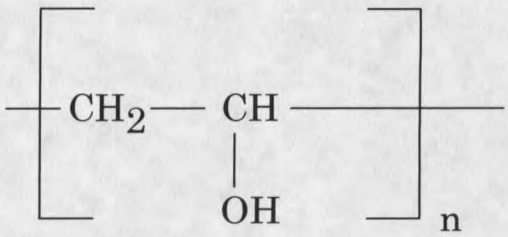

Figure 21. Reference polymer structures

Atomic concentrations of oxygen and carbon were measured by XPS and then compared to the theoretical values determined from the polymer stoichiometry and are shown in table 8.

	Theoretical Atomic Conc. (%)		Actual Atomic Concentration (%)			
Polymer ↓ Element →	C	O	C	O	F	Si
Poly(epoxy propyl methacrylate)	70	30	66.03	30.69	1.68	1.51
Poly(vinyl Alcohol)	66.7	33.3	66.03	33.97	0	0
Poly(acrylic acid)	60	40	60.65	39.35	0	0
Poly(vinyl methyl ketone)	80	20	80.03	19.97	0	0

Table 8. Reference polymer atomic concentrations

C1s curve deconvolution of the reference polymer spectra was used to compare peak areas for the different carbon-oxygen and carbon-hydrogen, carbon-carbon bonds to the expected values determined from polymer stoichiometry. The C-C, C-H component was numerically shifted to 285 eV with a corresponding shift in the C-O components. Figure 22 shows the poly(vinyl methyl ketone) C1s peak as an example. The bottom curve shows the fit curves and the data points and the top curve shows the summation of the fit curves overlaid on a line drawn though the data points to show how good the fit is.

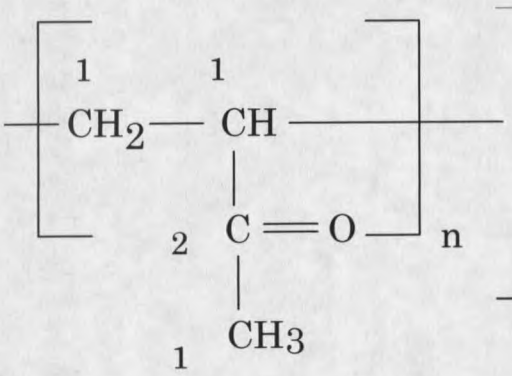

Peak Area Ratios	C-H, C-C	C-O
Carbon #	1	2
Stoichiometry	3	1
XPS results	3.3	1.0

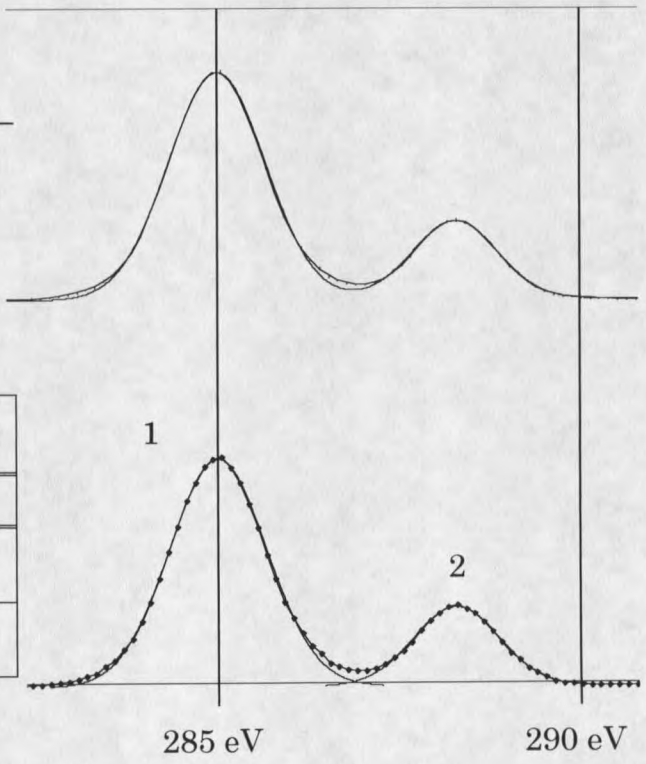

Figure 22. C1s spectra of poly(vinyl methyl ketone)

The monomer unit is composed of four carbon molecules one of which is doubly bound to an oxygen; therefore, the expected ratio of carbon bound to oxygen to carbon not bound to oxygen is 25% to 75% or a 1 to 3 peak area ratio. The first peak at 285 eV is from the carbons that are labeled with the number 1, and the second is from the carbon bound to oxygen labeled with the number 2. The peak areas work out to 23.2% to 76.8%, or a 1 to 3.3 ratio, reasonably close to the expected values. The remaining reference polymer C1s spectra are shown in figures 23, 24, and 25.

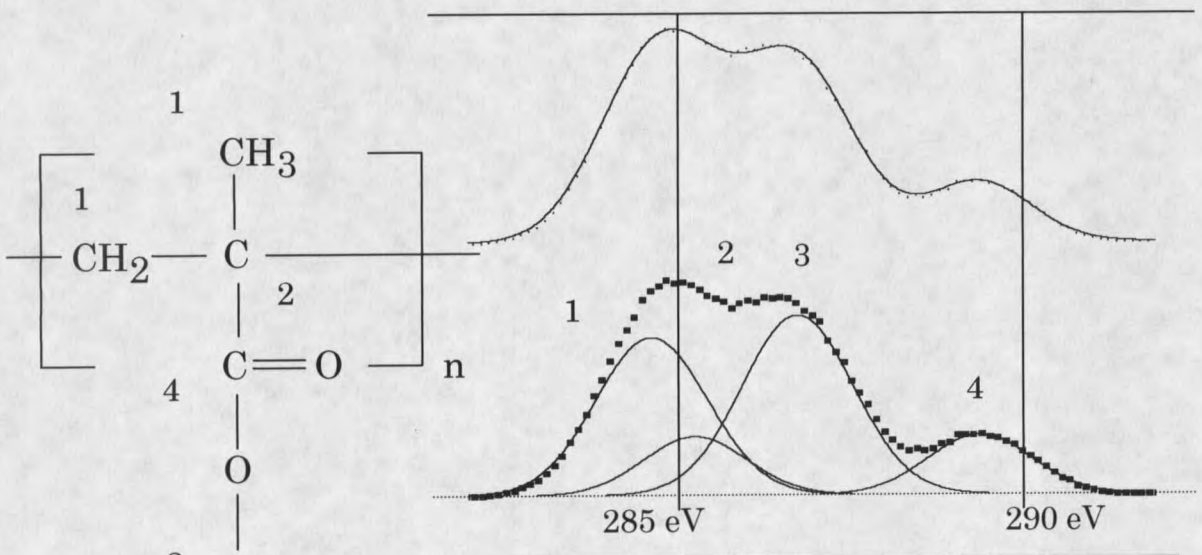

Peak Area Ratios	C-H, C-C	C-CO_2	C-O	O-C=O
Carbon #	1	2	3	4
Stoichiometry	2	1	3	1
XPS results	2.3	1	2.7	1

Figure 23. C1s spectrum of poly(epoxy propyl methacrylate)

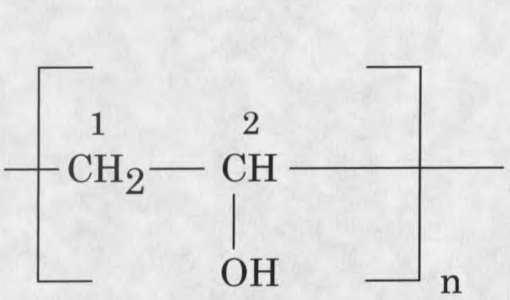

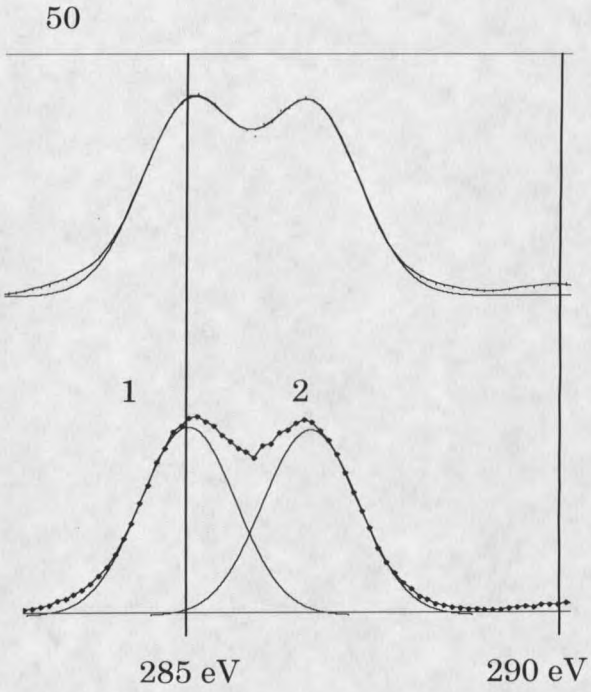

Peak Area Ratios	C-H, C-C	C-O
Carbon #	1	2
Stoichiometry	1	1
XPS results	1.0	1.0

Figure 24. C1s spectrum of poly(vinyl alcohol)

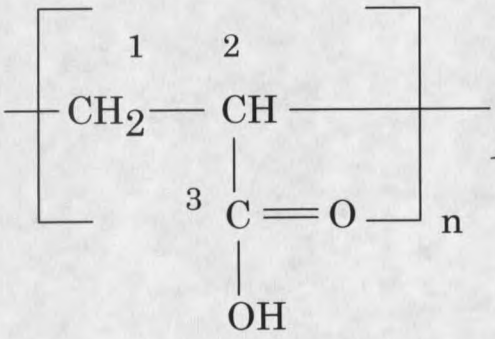

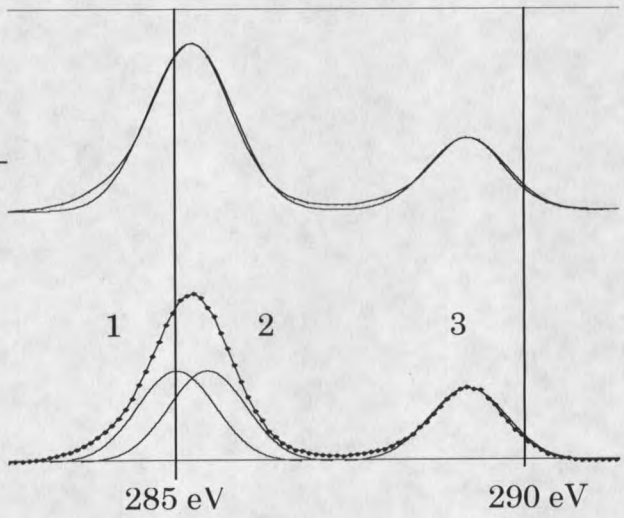

Peak Area Ratios	C-H, C-C	C-CO_2	O-C=O
Carbon #	1	2	3
Stoichiometry	1	1	1
XPS results	1.0	1.0	0.8

Figure 25. C1s spectrum of poly(acrylic acid)

These polymers fit about the same, with a less than 4% difference from theoretical values. The peak-fits are summarized in table 9.

Species → Polymer ↓	Theoretical Atomic Concentration (%)				Actual Atomic Concentration (%)			
	C-H, C-C	C-O	O-C=O or C=O	C-CO_2	C-H, C-C	C-O	O-C=O or C=O	C-CO_2
PEPMA	28.6	42.8	14.3	14.3	32.3	39.1	14.3	14.3
PAA	33.3		33.3	33.3	35.7		28.6	35.7
PVA	50	50			50.4	49.6		
PVMK	75		25		76.8		23.2	

Table 9. Reference polymer peakfit summary

The atomic concentrations in table 8 and the C1s peak fitting in table 9 indicate that the spin cast reference polymer surfaces were accurate as determined from the theoretical monomer stoichiometry.

Reference Polymer Derivatization

Each reference polymer was tested with each reagent for cross-reactions and extent of reaction. These data also helped to determine if the applicable reaction was occurring. Table 10 shows the atomic concentration of the applicable tag atom of each derivatizing agent with each reference polymer and an unmodified polystyrene sample. The reaction of each functional group and its intended derivatizing agent are shown in bold. The table shows that the reactions are fairly selective towards their intended

functional group, except that TFAA reacts significantly with epoxides. Hydrazine also reacts significantly with carboxylic acids.

Polymer→ ↓ Reaction	PVA Hydroxyls	PAA Carboxylic Acids	PVMK Ketones	PEPMA Epoxides	Control PS
TFAA	**32.7 % F**	0.6 % F	2.1 % F	25.4 % F	0.7 % F
TFE	0.33 % F	**24.4 % F**	0.91 % F	2.7 % F	0 % F
N_2H_2	2.4 % N	9.0 % N	**20.5 % N**	2.7 % N	0.2 % N
AcCl	<0.5 % Cl	<0.5 % Cl	<0.5 % Cl	**7 % Cl**	0.6 % Cl

Table 10. Derivatization cross-reaction summary

The C1s spectrum for poly(vinyl alcohol) after it has been exposed to trifluoroacetic anhydride is shown in figure 26 and table 11.

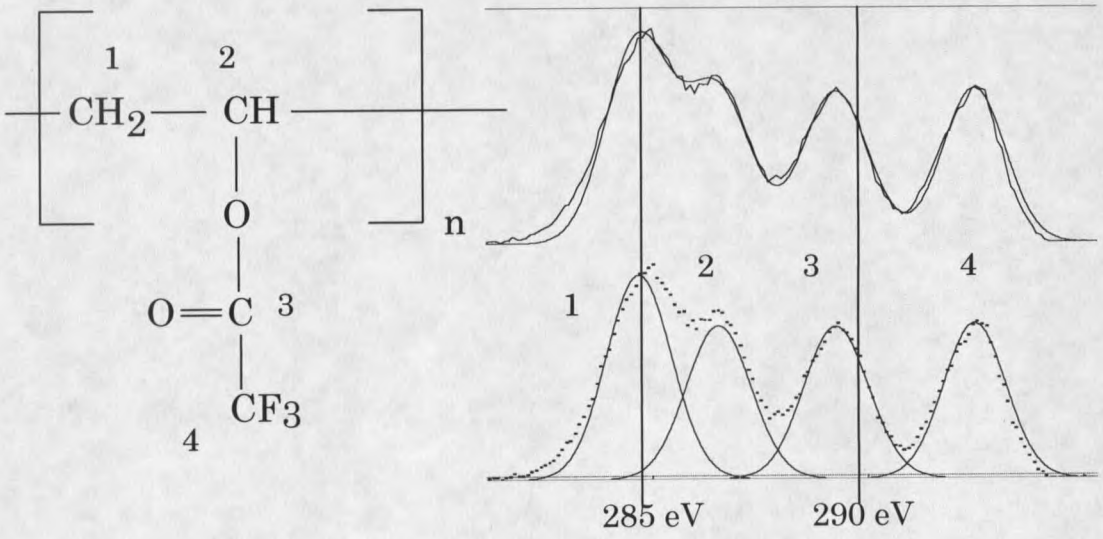

Figure 26. C1s spectrum of TFAA derivatized poly (vinyl alcohol)

Peak Area Ratios	C-H, C-C	C-O	O-C=O	CF_3
Carbon #	1	2	3	4
Stoichiometry	1	1	1	1
XPS results	1.2	1	1	1

Table 11. TFAA derivatized poly (vinyl alcohol) peak ratios

Trifluoroacetic anhydride was also found to react significantly with epoxides, even though a large amount of published literature implies the reaction is selective towards hydroxyls [21]. The suggested reaction scheme for this reaction is shown in figure 27 [21].

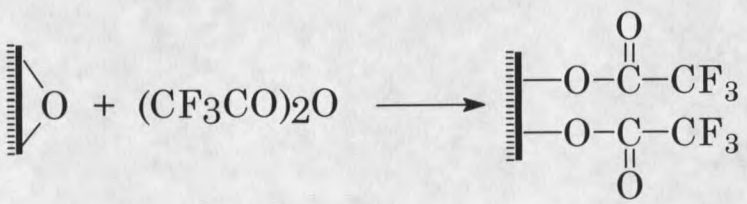

Figure 27. Trifluoroacetic anhydride and epoxide reaction.

The peak area ratios for the different carbons in the C1s spectra of TFAA derivatized poly(epoxy propyl methacrylate) are shown in figure 28 and indicate that the reaction in figure 27 is indeed occurring.

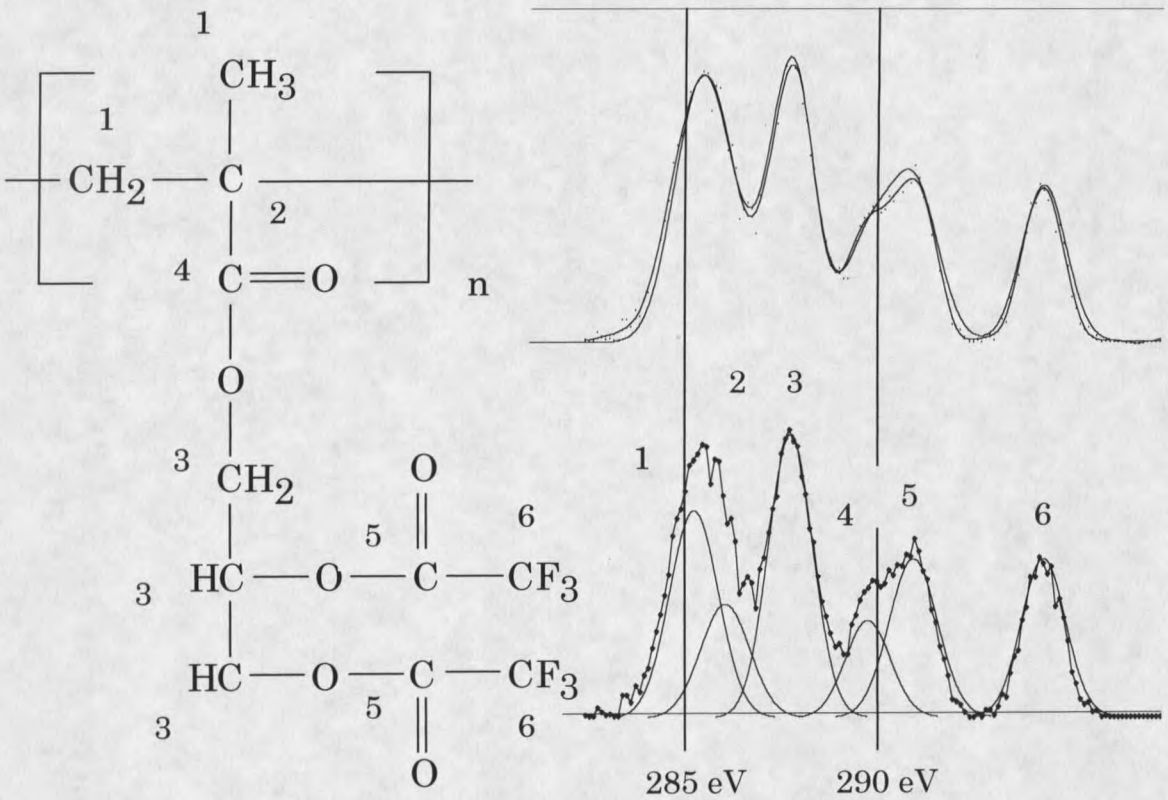

Peak Area Ratios	C-H, C-C	C-CO_2	C-O	O-C=O	CO_2-CF_3	CF_3
Carbon #	1	2	3	4	5	6
Stoichiometry	2	1	3	1	2	2
XPS results	2.1	1.3	2.9	1.0	1.8	1.6

Figure 28. C1s spectrum of TFAA derivatized poly (epoxy propyl methacrylate)

The C1s spectrum of acetyl chloride derivatized poly(epoxy propyl methacrylate) is shown in figure 29. There are two possible reaction products that could be envisioned. The chlorine atom could add to either carbon in the epoxide group, but because each possible structure has the same overall

number of carbon atoms in similar bonding environments, the two structures do not need to be taken into account when peak-fitting the C1s spectra. The peak area ratios match well to the theoretical values, indicating the reaction proceeds as envisioned.

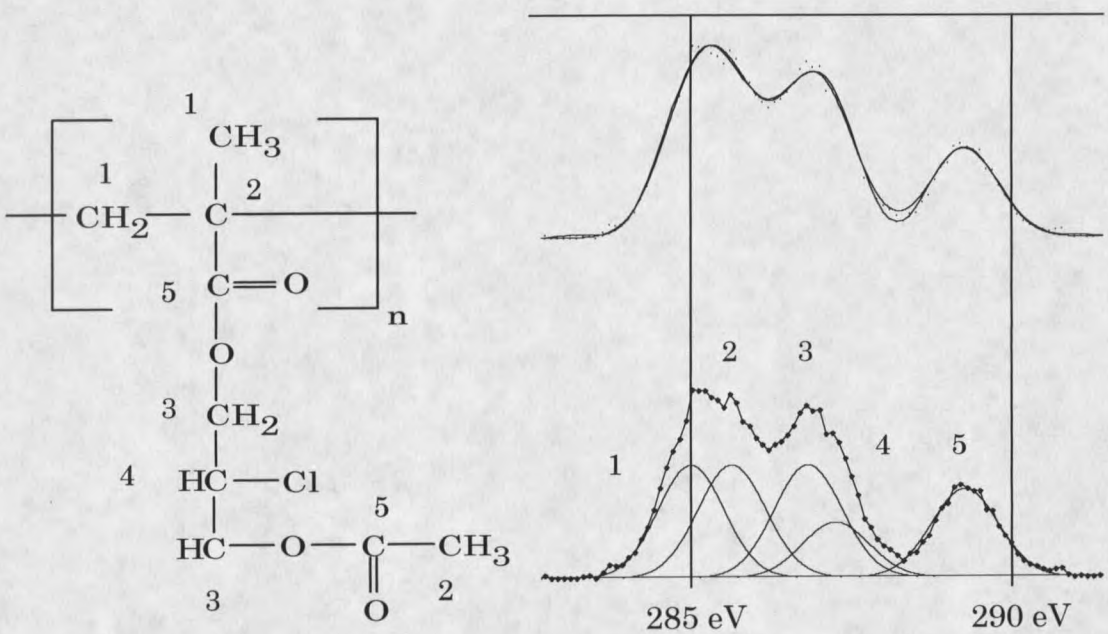

Peak Area Ratios	C-H, C-C	C-CO_2	C-O	C-Cl	O-C=O
Carbon #	1	2	3	4	5
Stoichiometry	2	2	2	1	2
XPS results	2.0	2.1	2.1	1.0	1.6

Figure 29. C1s spectrum of AcCl derivatized poly (epoxy propyl methacrylate)

The derivatization reaction for the carboxylic acid groups is the trifluoroethanol reaction series. The C1s spectrum of poly(acrylic acid) that has been derivatized with TFE is shown in figure 30. The expected peak area

ratios agree well with theoretical values, indicating that the reaction is occurring as planned.

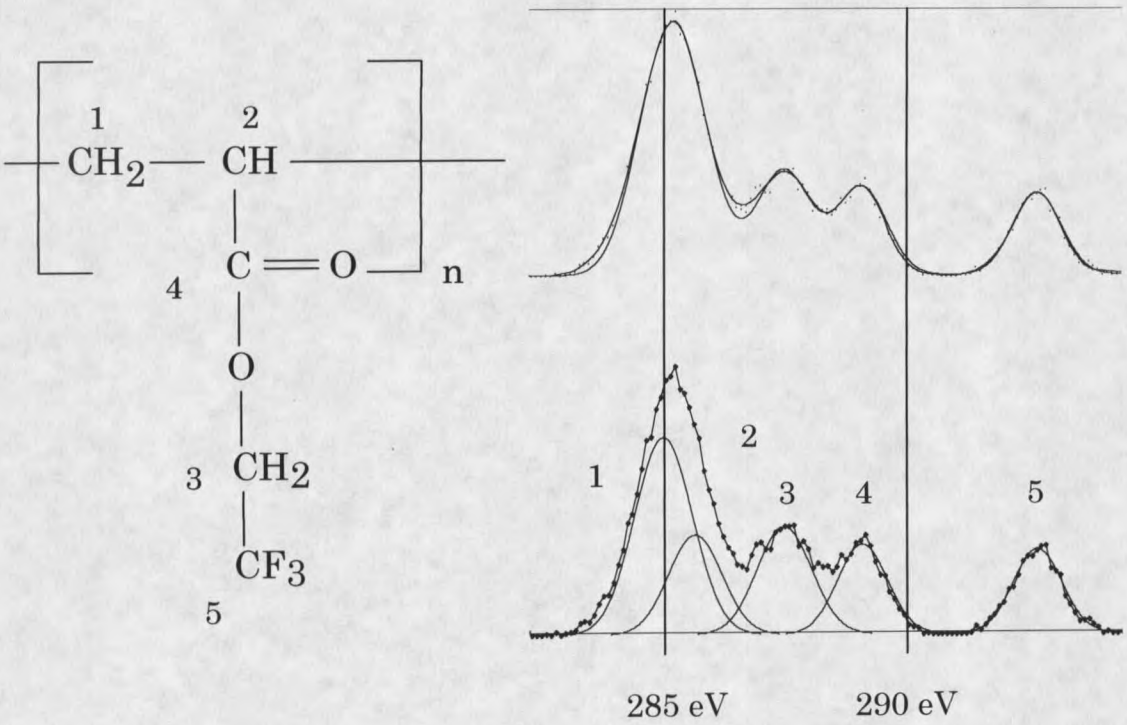

Peak Area Ratios	C-H, C-C	C-CO_2	C-O	O-C=O	CF_3
Carbon #	1	2	3	4	5
Stoichiometry	1	1	1	1	1
XPS results	1.9	0.9	1.0	0.8	0.7

Figure 30. C1s spectrum of TFE derivatized poly(acrylic acid)

The C1s peak deconvolution for the hydrazine derivatized poly(vinyl methyl ketone) is shown in figure 31. Due to the low binding energy shift of

C=N compared to C-C or C-H bond and the lack of obvious peaks, accurate C1s peak deconvolution is more problematic. The carbonyl peak at 288 eV indicates an incomplete reaction.

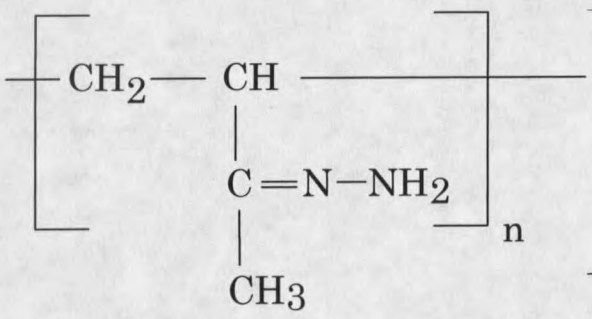

Peak Area Ratios	C-H, C-C	C=N	C=O
Peak #	1	2	3
Stoichiometry	3	1	0
XPS results	2.6	1.0	0.1

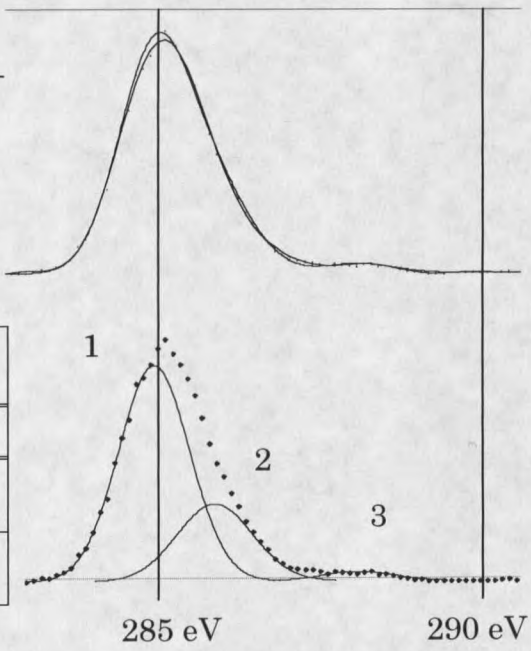

Figure 31. Hydrazine derivatized poly(vinyl methyl ketone)

Instead, greater emphasis must be placed on the overall carbon/nitrogen/oxygen (C/N/O) ratios to determine information about the reaction. The theoretical C/N/O ratios are 66.7/33.3/0.0 for the reaction. The actual ratios are 74.3/20.5/5.2. The fact that a significant amount of oxygen is still present as well as the lower than expected nitrogen concentration indicate that a significant amount of the ketone functionalities are not being derivatized.

The hydrazine also reacts significantly with poly(acrylic acid). The hydrazine is probably reacting with the acid group of poly(acrylic acid) as shown in figure 32.

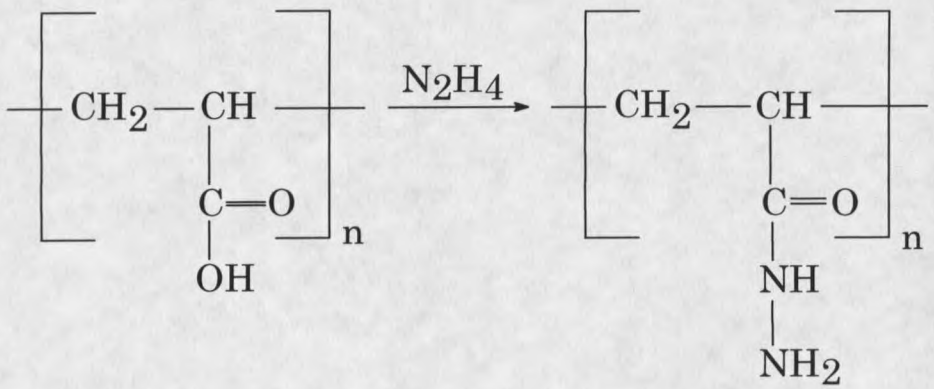

Figure 32. Hydrazine and poly(acrylic acid) reaction

Because the atomic concentration of nitrogen is only 9% and would be 33.3% for a complete stoichiometric reaction, there is a mixture of the product and the unreacted poly(acrylic acid). The binding energy of the carbon bound to the oxygen and nitrogen is only approximately 1 eV less than that of the carbon in the carboxylic acid. These conditions make peak fitting the C1s spectrum to determine if this reaction is occurring difficult. If the C1s spectrum of the hydrazine derivatized poly(acrylic acid) is overlaid on the unmodified poly(acrylic acid) C1s spectrum as in figure 33, only small differences can be seen between the spectra. The black trace is the underivatized PAA and the red trace is the derivatized PAA. If a close look is

taken at the carboxylic acid carbon peak at 289 eV, there is a suggestion of a peak on the left shoulder at approximately 288 eV. This peak is from the carbon bound to oxygen and nitrogen in the derivatized product. The 288 eV peak could also account for the overall slight decrease in binding energy for the peak.

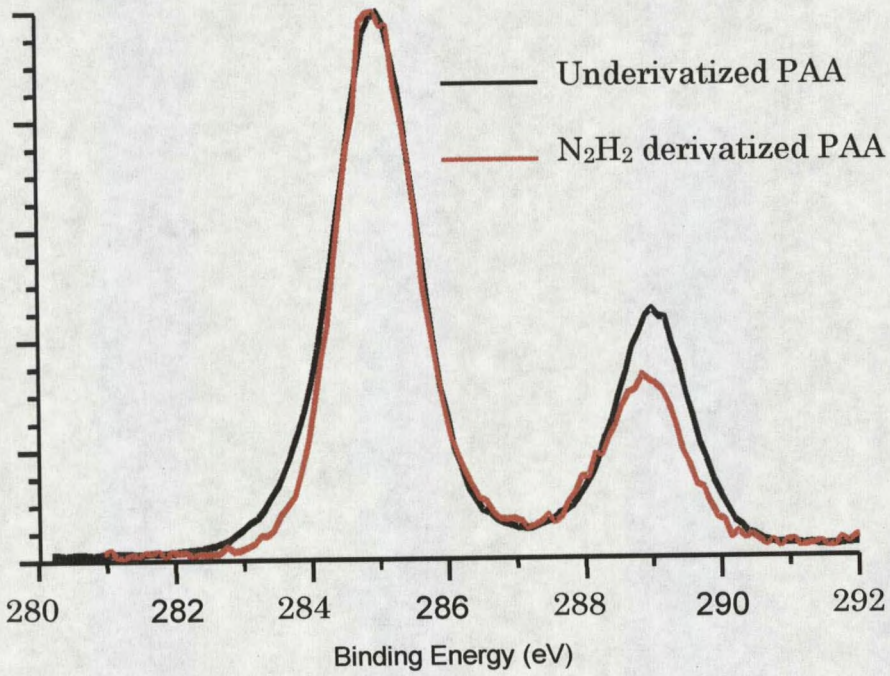

Figure 33. Hydrazine derivatized poly(acrylic acid)

After the reference polymers were derivatized, the reaction yield was calculated by taking the actual atomic concentration of the tag atom and dividing by the theoretical value and converting the result to percent. Table 12 summarizes the atomic concentrations and reaction yields.

Derivatizing Reagent and Polymer	Theoretical Atomic Concentration (%)			Actual Atomic Concentration (%)			Yield (%)
	C	O	F	C	O	F	
TFAA & PVA	44.4	22.2	33.3	45	22.3	32.7	98.2
TFAA & PEPMA	47.8	26.1	26.1	49.3	25.3	25.4	97.3
TFE & PAA	50	20	30	56.6	19	24.4	81.3
	C	O	Cl	C	O	Cl	
AcCl & PEPMA	64.3	28.6	7.1	66.2	26.8	7.0	98.6
	C	O	N	C	O	N	
N_2H_2 & PVMK	66.7	0	33.3	74.3	5.2	20.5	61.6

Table 12. Derivatization reaction atomic concentrations and reaction yields

Trifluoroacetic anhydride reacts mostly to completion with hydroxyls and epoxides. Acetyl chloride reacts mostly to completion with epoxides with no significant cross-reactions. The trifluoroethanol reagent series reacts with carboxylic acids to a lesser degree of 81% completion with no significant cross reactions. Hydrazine reacts to a much lower degree of completion of 62% with ketones and has a fairly significant reaction with carboxylic acids.

Modified Polystyrene Derivatization

The derivatization reactions were performed on the 100-pulse beam and 100 W plasma samples. The percentage of functional group in mol(functional group)/total surface moles was calculated by the method

described in chapter 2 for each reaction. The TFAA reaction lists two values, one calculated as all hydroxyls and the other calculated as all epoxide since the reaction labels hydroxyls with three fluorine atoms and the epoxides are labeled with 6 fluorine atoms. The results are shown in Table 13.

	100 pulse Beam Sample (%)		100 W Plasma Sample (%)	
	All OH	All Epoxide	All OH	All Epoxide
Hydroxyls TFAA	4.02	2.05	4.11	2.10
Carboxylic Acids TFE	0.73 x2 = 1.46		.88 x2 = 1.76	
Carbonyls N_2H_2	4.6		3.1	
Epoxides AcCl	5.2		4.2	
Sums for A.C comparison	15.3		13.2	
Total A.C. oxygen (XPS)	16.8		15.2	

Table 13. Derivatization summary on modified samples

If it is assumed that the reactivities are the same as the reactivities for the reference polymers, the new functional group percentages are shown in table 14.

	100 pulse Beam Sample (%)		100 W Plasma Sample (%)	
	All OH	All Epoxide	All OH	All Epoxide
Hydroxyls TFAA	4.1	2.1	4.2	2.2
Carboxylic Acids TFE	0.90 x2 = 1.8		1.1 x2 = 2.2	
Carbonyls N_2H_2	7.5		5.0	
Epoxides AcCl	5.3		4.3	
Sums for A.C comparison	18.7		15.7	
Total A.C. oxygen (XPS)	16.8		15.2	

Table 14. Derivatization summary with reaction yield data

Surface Topography

Surface topography was examined on the one year old modified samples with Atomic Force Microscopy and Scanning Electron Microscopy. Figure 34 shows scanning electron micrographs of the 10, 100, 1000, 10,000 pulse, and unmodified polystyrene samples. Figure 35 shows the 100 and 180 W plasma samples. The images are at a magnification of 40,000 looking normal to the surface. Note the increase in the number of similarly sized sub-micron surface features as the beam exposure increases while the plasma sample shows no change in surface roughness relative to the unmodified sample. AFM analysis indicates that the features are nominally 10 to 15 nanometers

in height and 50 to 75 nanometers in width. The AFM SEM, and previous XPS data, indicate that the sub-micron surface roughness can be varied while maintaining nearly constant surface chemistry on oxidized polystyrene surfaces.

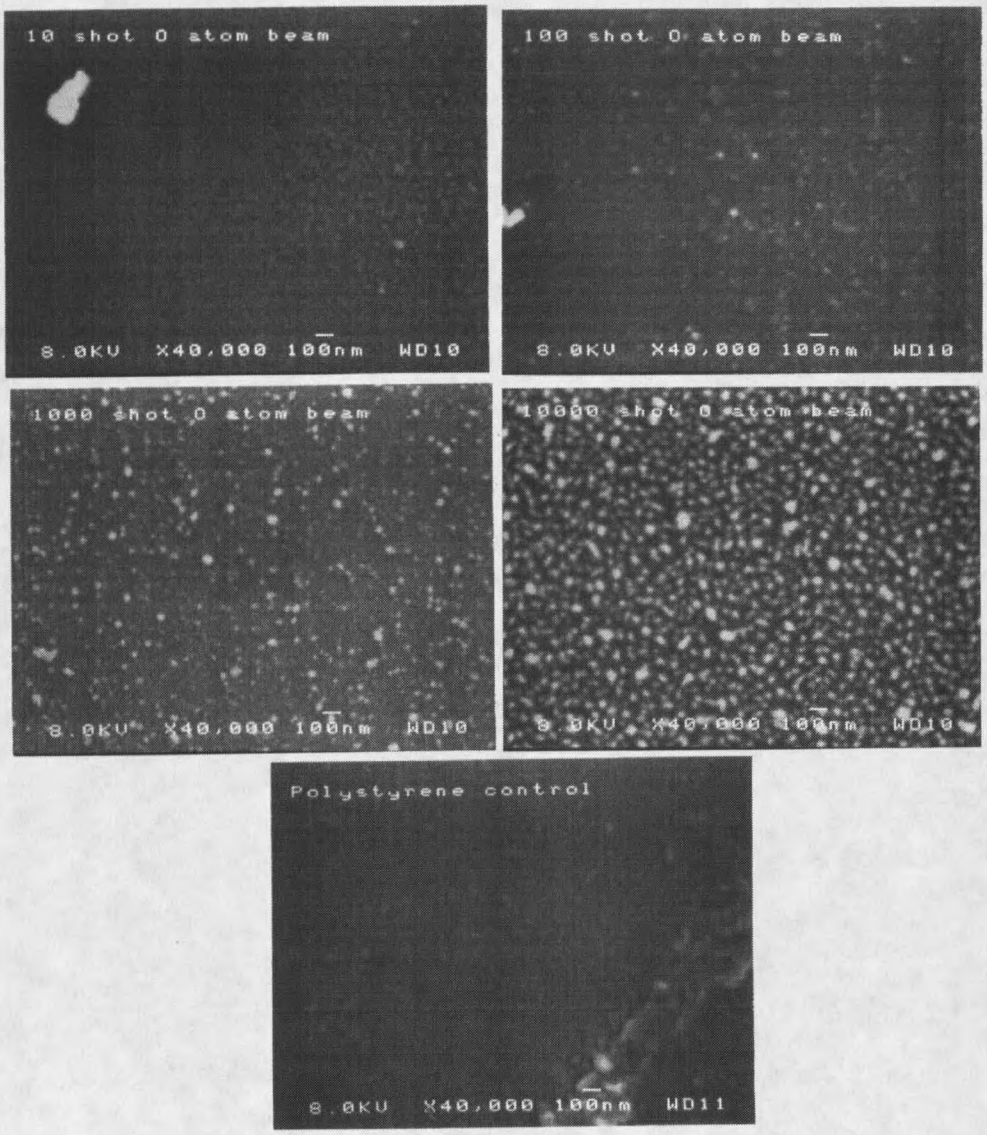

Figure 34. SEM images of the beam treated samples

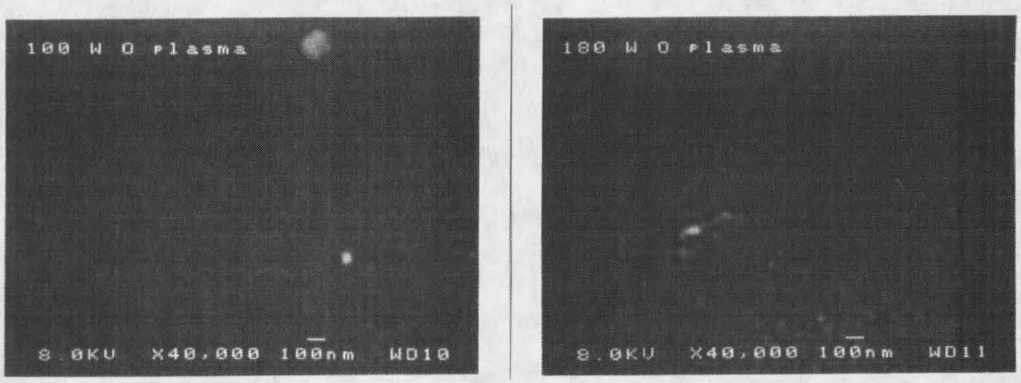

Figure 35. SEM images of the plasma treated samples

CHAPTER 4

DISCUSSION AND CONCLUSIONS

Discussion

Curve Deconvolution

Accurate curve deconvolution presents a number of problems. First, a number of carbon-oxygen functionalities overlap in binding energy. Second, a specific functionality can occur over a range of up to one eV when it occurs in different chemical structures. Lastly, it is rather simple to perfectly curve fit a spectrum, but rather more difficult to say that a fitted peak corresponds to something real on a surface that has a variety of functionalities in low concentrations such as the modified surfaces in this study.

Peak fitting the beam modified sample spectra in the conventional manner does not work. The unconventional manner in which the surfaces were fit with a peak at 2.0 eV and the singly bound oxygen peak at 1 eV was necessary for good fits of the beam modified samples. The exact chemical nature of this peak is undetermined at this time although the peak is labeled as an epoxide. The exact chemical nature of the peak at ~5 eV is also undetermined at this time even though the literature labels carbon-oxygen

peaks of this energy as carbonates. Whatever the origin of the peaks with binding energy shifts of 2 and 5 eV, the fact that they decay with time cannot be overlooked.

The plasma modified C1s spectra were fit with the same parameters to provide a direct comparison of the beam and plasma modified spectra even though none of the literature on plasma or photo-oxidized polystyrene perform curve fits with a peak at 2.0 eV. Although the plasma spectra fit very well with this fitting scheme, it may not be valid for the plasma-modified surfaces.

Surface Oxidation

The surface modification methods of plasma and molecular beam exposure produce similar overall oxygen content, although it appears that the long-duration beam exposure tends to oxidize the surface somewhat more than the most intense plasma treatment. A remarkable observation is that the oxygen atomic concentrations on the beam-treated samples increased by less than 50 percent when the incident atomic oxygen fluence increases by three orders of magnitude. Surface oxidation seems to approach steady state rapidly during the initial attack from the first few monolayers of impinging O atoms.

Both the plasma and beam treated samples exhibit strongly asymmetric peak shapes with higher binding energy components relative to

an unmodified surface, indicating a wide range of carbon-oxygen bonding environments on the treated surfaces. However, the difference in shape of the curves for the modified surfaces suggests that the distribution of carbon-oxygen bonding environments is different between the two methods.

When the samples were reanalyzed after one year, the plasma modified surfaces showed a much lower decrease in oxygen and were essentially unchanged. The beam modified samples, especially the 10,000 pulse exposure, showed a much greater loss of surface oxygen. The loss appeared to be concentrated in the unidentified peaks at 2.0 eV and 5 eV that were labeled as an epoxide and a carbonate. These species were shown to last up to two weeks. Once this loss occurred, the beam modified samples remained stable. Work is continuing within the research group to positively identify these metastable species. After the beam treated samples degraded, the different durations of exposure had similar overall oxygen content with similar chemistry.

The plasma exposed surfaces showed a progressive loss of aromaticity with total loss of the aromatic character in the 180 W sample. Apparently, the plasma treatment destroys the aromatic character throughout the surface layer probed by XPS. The preservation of aromatic character in the beam treated surface suggests a reduced reactivity of the beam with the aromatic ring. Table 6 shows a loss of the aromaticity in the beam exposed surfaces, which is not apparent from looking at the spectra. This may well be an

artifact of the peak fitting process. Similar overall changes in the intensity of the $\pi \rightarrow \pi^*$ satellite in the beam modified samples are readily apparent from the spectra.

Derivatization Reactions

Tables 15 and 16 illustrate a big inconsistency in the data. In an ideal situation the value obtained from the TFAA should be the sum of the hydroxyls and epoxides with some distribution between the two moieties. This value should be greater than that obtained from the AcCl reaction which is the epoxide concentration only. It is not. In the case of no hydroxyls being present, the values from the TFAA and AcCl reactions should be consistent with each other. They are not. In other words, the fluorine concentration should be significantly higher than it is on the modified samples with the TFAA reaction. This indicates that reactivity for the TFAA reaction on both epoxides and hydroxyls is significantly reduced at low concentrations of functional groups. A study of the TFAA reaction in a poly(styrene/hydroxystryrene) copolymer series found that the hydroxyl groups were stoichiometrically tagged only when their concentrations were greater than 4% [24]. This is not ideal for plasma or beam treated polymer surfaces where the hydroxyl concentration is expected to be only a fraction of the total oxygen content on the surface. The other derivatization reactions

may have similar concentration concerns that need to be investigated before this technique can be used for accurate quantization in mixed systems.

Additional Hydroxyl Derivatization Reactions

Because of the problems with the TFAA reaction in the presence of hydroxyls and epoxides, different reactions were investigated to derivatize hydroxyls. Vapor phase hydroxyl derivatization reactions with thionyl chloride and phosphorus trichloride were investigated. These possible reactions were determined by discussions with organic chemists and investigation of an organic chemistry text [25]. The thionyl chloride and phosphorus trichloride liquid phase reactions as used by organic chemists are shown in figure 36.

$$R{-}OH + SOCl_2 \xrightarrow{\text{Pyridine}} R{-}Cl + SO_2 + HCl$$

$$3R{-}OH + PCl_3 \longrightarrow 3R{-}Cl + H_3PO_3$$

Figure 36. Textbook reactions

The thionyl chloride reaction was tried as envisioned with various procedures similar to the other derivatization reactions with various times and temperatures on the poly(vinyl alcohol) reference polymer. The reaction

was also tried without the pyridine to obtain an intermediate from the textbook reaction. This reaction is shown in figure 37.

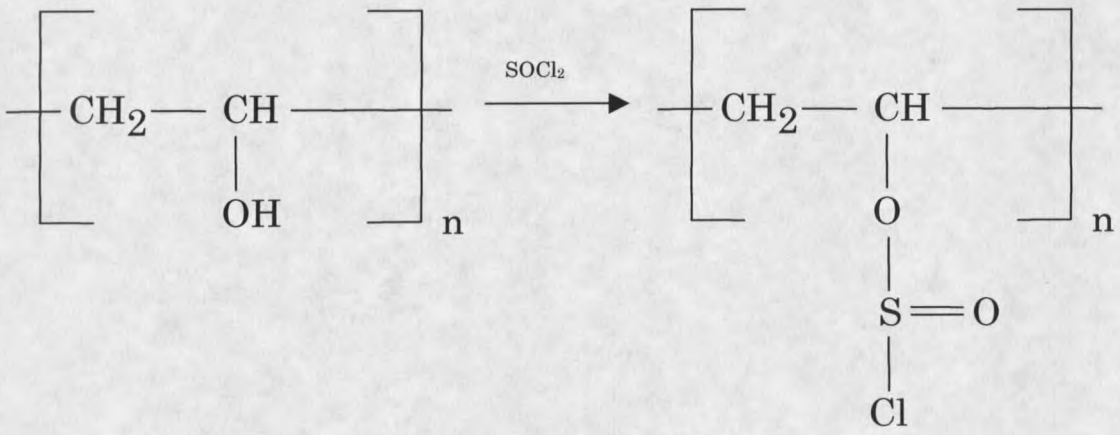

Figure 37. Thionyl chloride and poly(vinyl alcohol) reaction

The results were inconclusive with about 52-57% carbon, 28-32% oxygen, 7-11% sulfur, and 1-5% chlorine. Clearly, there wasn't a consistent stoichiometric reaction occurring that could be useful for hydroxyl derivatization, so no further work was done.

When poly(vinyl alcohol) was exposed to phosphorus trichloride vapor at 50^{0}C for one hour in the same procedure as the TFAA hydroxyl derivatization, some interesting results were obtained. The C/O/P ratio came out to be 31.74/52.24/16.02. These results are very close to a possible product having one phosphorus atom, two carbon atoms, and three oxygen atoms. In

the liquid-phase alcohol-phosphorus trichloride textbook reaction, the first step is shown in figure 38 for poly(vinyl alcohol).

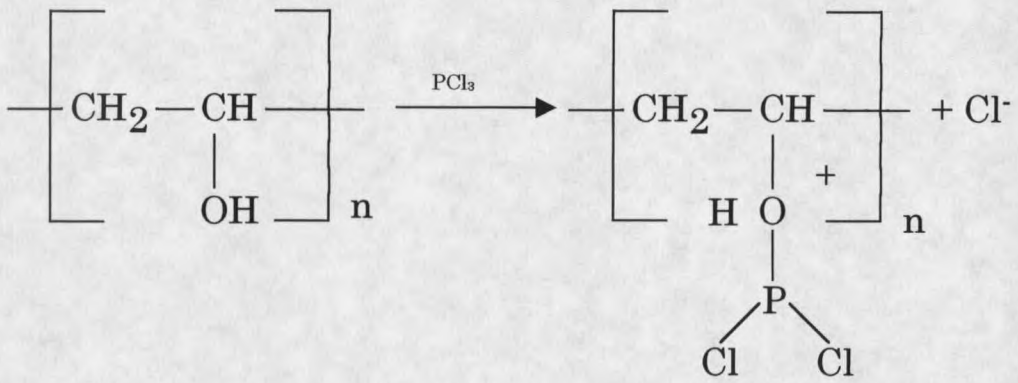

Figure 38. Textbook liquid phase PVA and PCl_3 reaction step

The next step would be from a chloride ion acting as a nucleophile and displacing the $HOPBr_2$ group. From the C/O/P ratios that were obtained, the possible structure shown in figure 39 was determined.

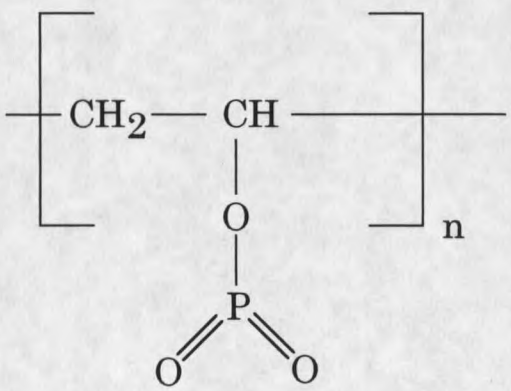

Figure 39. Theoretical PVA and PCl_3 reaction product

At the time, it was determined that there wasn't a reasonable way for this product to be occurring. No further work was done on the reaction. After a conversation with Dr. Cynthia McClure of MSU-Bozeman who is very knowledgeable of phosphorus chemistry, it was determined that the product in figure 36 could quite likely be occurring. The reaction was attempted again, but because of about 8% Si contamination in the poly(vinyl alcohol) films that were made and the fact that the phosphorus trichloride had not been stored under nitrogen properly and was about seven months old and was probably bad, inconclusive results were obtained. Further work needs to be done on this reaction with good films and fresh phosphorus trichloride. If this reaction is occurring, it could be useful as a derivatization agent to separate hydroxyls and epoxides since the PCl_3 should not react with an epoxide. There was not enough time for further work for inclusion in this thesis.

Conclusions

Surface Oxidation

The two surface modification methods produced clear differences in surface functional group distribution with similar overall oxygen content. A steady state occurred early on during the beam exposures. The beam exposure produced metastable species that lasted up to two weeks. Once

these species had degraded, the surface chemistry (as measured by XPS) was nearly identical for the different beam exposure durations. The plasma-modified samples were nearly unchanged after one year. Surface roughness with sub-micron features increased proportionally with beam exposure duration while the plasma exposure did not effect surface roughness. In other words, sub-micron surface roughness could be varied independently of surface chemistry on the beam treated polystyrene. The 180 W plasma exposure resulted in complete destruction of the aromatic character of the polymer within the sampling depth of XPS while the beam did not damage the aromatic character of the sample.

Surface Derivatization

The two functional group analytical techniques of surface derivatization and C1s curve deconvolution did not agree quantitatively on low concentration mixed functionality systems like the modified surfaces. They worked well on for analysis of the reference polymers where there are large concentrations of a specific functionality. The derivatization technique needs further investigation for certain functionalities or combinations of functionalities to obtain quantitative results on systems with more than two components. They did not work quantitatively for the systems in this study.

REFERENCES

1. W. Reitz, "The Critical Role of Surface Modification in Biomaterials," The Journal of the Minerals, Metals, and Materials Society, 49(2) (1997) 44

2. M. Mouka, "The Development of Polymer-Based Biomaterials Since the 1920's," The Journal of the Minerals, Metals, and Materials Society, 49(2) 46-51

3. U. Plawky, M. Londschien, and W. Michaeli, "Surface Modification of an Aramid Fibre Treated in Low-Temperature Microwave Plasma," Journal of Materials Science, 31 (1996) 6043-6053

4. W. G. Collier and T. P. Tougas, "Determination of Surface Hydroxyl Groups on Glassy Carbon with X-ray Photoelectron Spectroscopy Preceded by Chemical Derivatization," Analytical Chemistry 59 (1987) 396-399

5. D. Briggs, Surface Analysis and Pretreatment of Plastics and Metals, ed. D. M. Brewis, (New York, Macmillan Publishing Co., Inc., 1982)

6. R. K. Wells, J. P. S. Badyal, I. W. Drummond, F. J. Street, and K. S. Robinson, "Plasma Oxidation of Polystyrene vs. Polyethylene," Journal of Adhesion Science and Technology, 7(10) (1993) 1129-1137

7. A. G. Shard and J. P. S. Badyal, "Surface Oxidation of Polyethylene, Polystyrene, and PEEK: The Synthon Approach," Macromolecules 25 (1992) 2053-2054

8. R. K. Wells, J. P. S. Badyal, I. W. Drummond, F. J. Street, and K. S. Robinson, "A comparison of Plasma-Oxidized and Photo-Oxidized Polystyrene Surfaces," Polymer 34(17) (1993) 3611-3613

9. A. G. Shard and J. P. S. Badyal, "Plasma Oxidation versus Photooxidation of Polystyrene," Journal of Physical Chemistry, 95 (1991) 9436-9438

10. P. C. Schamberger, J. I. Abes, and J. A. Gardella, Jr., "Surface Chemical Studies of Aging and Solvent Extraction effects on Plasma treated Polystyrene," Colloids and Surfaces B: Biointerfaces," 3 (1994) 203-215

11. E. Occhiello, M. Morra, P. Cinquina and F. Garbassi, "Hydrophobic Recovery of Oxygen-Plasma-Treated Polystryrene," Polymer, 33(14) (1992) 3007-3015

12. J. D. Andrade, Surface and Interfacial aspects of Biomedical Polymers, ed. J. D. Andrade (New York, Plenum Press, 1985), chap. 5

13. B. D. Ratner and D. G. Castner, Surface Analysis: Techniques and Applications, ed. J. C. Vickerman and N. M. Reed (Chichester, UK: John Wiley and Sons, 1992), 151-218

14. G. Beamson and D. Briggs, High resolution XPS of Organic Polymers-The Scienta ESCA300 Database (New York: John Wiley & Sons, 1992), appendix 1, chap 2,8

15. D. Fang, M. S. Thesis, Montana State University-Bozeman, 1996

16. C. F. Quate, "The AFM as a Tool for Surface Imaging," Surface Science, 299/300 (1994) 980-995

17. G. E. Caledonia, R. H. Krech, and B. D. Green, AIAA J. 25 (1987) 59

18. Y. T. Lee, J. D. McDonold, P.R. LeBreten, and D. R. Herschlach, "Molecular Beam Reactive Scattering Apparatus with Electron Bombardment Detector," The Review of Scientific Instruments, 40, (1969) 1402-1408

19. R. K. Sparks, Ph. D. thesis, University of California, Berkeley (1980)

20. K. P. Giapis, T. A. Moore, and T. K. Minton, Journal of Vacuum Science and Technology A, 13 (1995) 959

21. A. Chilkoti and B. D. Ratner, "An X-ray Photoelectron Spectroscopic Investigation of the Selectivity of Hydroxyl Derivatization Reactions," Surface and Interface Analysis 17 (1991) 567-574

22. A. Chilkoti, B. D. Ratner, and D. Briggs, "Plasma-Deposited Polymeric Films Prepared from Carbonyl-Containing Volatile Precursors: XPS Chemical Derivatization and Static SIMS Surface Characterization," Chemistry of Materials 3 (1991) 51-61

23. J. A. Gardella, Jr., S. A. Ferguson, and R. L. Chin, "$\pi^* \leftarrow \pi$ Shakeup Satellites for the Analysis of Structure and Bonding in Aromatic Polymers by X-ray Photoelectron Spectroscopy," Applied Spectroscopy 40(2) (1986) 224-232

24. A. Chilkoti, D. G. Castner, B. D. Ratner, and D. Briggs, "Surface Characterization of a Poly(styrene/ρ-hydroxystryrene) Copolymer Series using X-ray Photoelectron Spectroscopy, Static Secondary Ion Mass Spectrometry, and Chemical Derivatization Techniques," Journal of Vacuum Science and Technology A 8(3) (1990) 2274-2282

25. T. W. G. Solomons, Organic Chemistry, (New York: John Wiley & Sons, 1992), 425, 426, 775,776

26 C. N. Reilly, D.N. Evenhart, and Floyd F.-L Ho, Applied Electron Spectroscopy for Chemical Analysis, ed. W. Hassan and Floyd F.-L Ho, (New York, John Wiley and Sons, 1982), chap. 6

27 S. Yuan and R. E. Marchant, "Surface modification of Polyethylene Film by Plasma Polymerization and Subsequent Chemical Derivatization," Journal of Applied Polymer Science: Applied Polymer Symposium 54 (1994) 77-91

28 J. A. Lanauze and D. L. Myers, "Ink Adhesion on Corona-Treated Polyethylene Studied by Chemical Derivatization of Surface Funtional Groups," Journal of Applied Polymer Science, 40 (1990) 595-611

29 D. C. Schram, Th. H. J. Bisschops, G. M. W. Kroesen, and F. J. de Hoog, "Plasma Surface Modification and Plasma Chemistry," Plasma Physics and Controlled Fusion, 29(10A) (1987) 1353-1364

30 D. E. Brinza, ed., "NASA Workshop on Atomic Oxygen Effects," JPL Publication 87-14 (Pasadena, CA. 1987)

31 M A. Golub, T. Wydeven, and R. D. Cormia, "ESCA Study of Several Fluorocarbon Polymers Exposed to Atomic Oxygen in Low Earth Orbit or Within or Downstream from a Radio-Frequency Oxygen Plasma," Polmer, 30 (1989) 1571-1575

32 T. K. Minton, JPL Publication **94-02** (Pasadena, CA. 1994)